

The Effects of Testosterone on Protein Expression in C2C12 Myoblasts During Differentiation

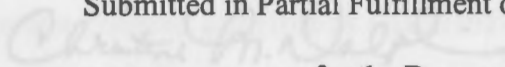
Christine M. Dolphin

I hereby release this thesis to the public. I understand that this thesis will be made available from the Ohio LINK ETD Center and the Maag Library Circulation Desk for public access. I also authorize the OhioLINK ETD Center to make copies of this thesis as needed for scholarly research.

Christine M. Dolphin

Signature:

Submitted in Partial Fulfillment of the Requirements



7/29/05

Christine M. Dolphin, Student

for the Degree of

Date

Master of Science

Approval:

in the



Biological Sciences

7/29/05

Dr. Gary R. Walker, Thesis Advisor

Date

Program



7/29/05

Dr. David K. Asch, Committee member

Date



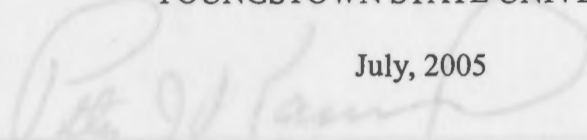
7/29/05

Dr. Chester R. ...

Date

YOUNGSTOWN STATE UNIVERSITY

July, 2005



8/9/05

Dr. Peter J. Kasvinsky, Dean of Graduate Studies

Date

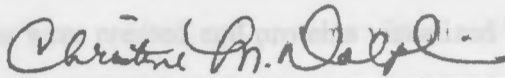
The Effects of Testosterone on Protein Expression in C2C12 Myoblasts

During Differentiation

Christine M. Dolphin

I hereby release this thesis to the public. I understand that this thesis will be made available from the Ohio LINK ETD Center and the Maag Library Circulation Desk for public access. I also authorize the University or other individuals to make copies of this thesis as needed for scholarly research.

Signature:

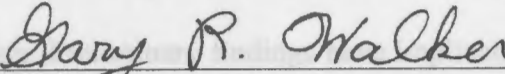


7/29/05

Christine M. Dolphin, Student

Date

Approvals:



7/29/05

Dr. Gary R. Walker, Thesis Advisor

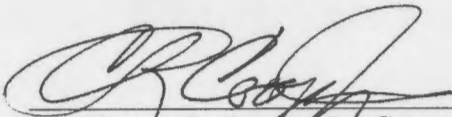
Date



7/29/05

Dr. David K. Asch, Committee member

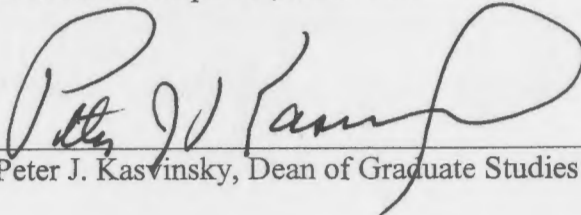
Date



7/29/05

Dr. Chester R. Cooper Jr., Committee member

Date



8/9/05

Dr. Peter J. Kasvinsky, Dean of Graduate Studies

Date

Abstract

The underlying cellular mechanisms of postnatally-derived stem cells known as myoblasts have been examined to aid in the advancement of reparative and regenerative-type therapies for diseases such as muscular dystrophy. This study focused on myogenic differentiation, a process in which immature myoblasts fuse to form mature, contractile myotubes and irreversibly withdraw from the cell cycle in response to muscle-regulatory proteins. The C2C12 cell line provided the means for studying differential proteins linked to muscle development. C2C12 cells were cultured under appropriate sterile conditions and harvested in a time-dependent manner. Harvested samples were then subjected to quantitative protein analysis and two-dimensional gel electrophoresis (2DGE) in which protein maps were created and proteins visualized by Coomassie Brilliant Blue stain and highly sensitive SYPRO[®] Ruby protein gel stain. The anabolic compound testosterone was administered to myogenic cultures to determine the effects of testosterone on gene expression and the proteome of these myogenic cells during the process of differentiation. Preliminary findings have implicated differential proteins at various time points, indicating changes in gene expression. Future work will be carried out to determine the amino acid sequences and thus the identity of testosterone induced proteins.

Acknowledgements

Throughout the last year at State University, I have had the

Table of Contents

Abstract.....iii

Table of Contents.....iv

Acknowledgements.....v

List of Tables.....vi

List of Figures.....vii

Dr. Walker, I truly appreciate all of the time and devotion you have so freely offered to my project and I. Always with a smile, you have never faltered in your goal of keeping us on task, almost an impossible feat. I'd also like to thank you for always taking a sincere interest in the lives of all of us in the lab, no matter how crazy the story.

Chapters

Chapter **Page**

I. Introduction.....1

II. Materials and Methods.....27

III. Results.....42

IV. Discussion.....84

V. References.....88

Chandler, Don Brown, Erin Truitt, Kiran, Irah, and Nadima. Special thanks to Pat and Davis for being so nice about my annoying office requests. Thanks to Mary. Thank you Dr. Fagan for all that you have taught me. Thank you to Dr. Jill Tall for being such a good friend. Thank you Dr. Benya for your kindness. Thank you to Dr. Womble for allowing me this opportunity, and for your time and effort in organizing all of the crazy

Acknowledgements

Throughout the last two years at Youngstown State University, I have had the fortunate opportunity of encountering many wonderful people along the way. The journey has been slow and steady, yet inexplicably rewarding. Like many scientists, I have encountered several setbacks and discouragements. Yet somehow those only contribute to the feelings of self-fulfillment and accomplishment I have gained. It feels great to have finally made it!

Dr. Walker, I truly appreciate all of the time and devotion you have so freely offered to my project and I. Always with a smile, you have never faltered in your goal of keeping us on task, almost an impossible feat. I'd also like to thank you for always taking a sincere interest in the lives of all of us in the lab, no matter how crazy the story. Most importantly, thank you for your infinite knowledge and guidance, and always making life fun. I would also like to thank my committee members Dr. Cooper and Dr. Asch. Dr. Cooper, thank you for your contagiously-positive attitude and your time contributed to reading this long thesis, not during vacation. Dr. Asch, thank you for always being so simultaneously smart and cool about the everyday occurrences of life.

There are many other people without whom this would not be possible. Thank you to everyone in the Proteomics Research Group for all your help: Dr. Kim, Julie Chandler, Don Brown, Erin Treece, Kiran, Balu, and Neelima. Special thanks to Pat and Travis for being so nice about my annoying office requests. Thanks to Mary. Thank you Dr. Fagan for all that you have taught me. Thank you to Dr. Jill Tall for being such a good friend. Thank you Dr. Benyo for your kindness. Thank you to Dr. Womble for allowing me this opportunity, and for your time and effort in organizing all of the crazy

Grad students. (minus my last teaching schedule!) Thank you Dr. Diggins for our friendly hallway-talks and popcorn. Thank you Dr. Leipheimer and Dr. Toepfer for passing on your knowledge. Thank you Dr. Bruce Waller and Dr. Palmer-Fernandez for treating us as equals.

Special thanks to my wonderful lab buddies whom without I would have lost my sanity. Thank you Steve Robbins for always being there for me, Lisa Zelinka for our talks, Dr. Tom Watkins for your sense of humor, Kyle Sobecki for making it through together, and both Chet Cooper Chris Breen for making the last two years fly by. I love you guys and I will miss you very much. Special thanks to my office buddies for being such wonderful and supportive friends Tammy D iglaw, Becky Rupert and Lisa Tarcy. Thank you also to all my fellow grad students. Special thanks to all my work buddies.

I'd also like to thank Kathleen and Craig Dolphin, my Mom and Dad. I couldn't have possibly made it through this many years of school without their love and support. Special thanks to Anne M. Schuler, my Grandma, for being such a strong and influential woman. Thanks to all of my aunts, uncles, and cousins. Special thanks to my Godparents Mike and Margie Kolich. Thank you to all of my family members for making life sweeter: Kathleen, Mike and Nathan Soubeyrand, Carolyn, Jerry, Cierra, and Gianna Latronica, Rich, Jill and Jesse James Dolphin, Cheryl and John Gentile, Jeffrey, Dianne and Patrick Dolphin. I love you all. Also, thank you Johnny for teaching me everything you know. Thank you to my best friend forever, Faith. Thank you to Mama B, Nena, Matt, Bill, Leon and my Noah for your kindness. I saved the best for last...I like to thank my Stevie for never giving up on me. Thank you for the way you always love and take care of me. We're one step closer!

List of Tables

Table	Page
Table 2.1 Polyacrylamide Gel Components.....	41
Table 3.1 Modified Bradford Assay Concentrations and Absorbances.....	48
Table 3.2 Sample Protein Concentrations.....	52
Figure 1.4 Myogenic Differentiation Pathways.....	17
Figure 1.5 Components of the Cell-Cycle Control System.....	23
Figure 2.1 Two-Dimensional Gel Electrophoresis.....	29
Figure 3.1 Standard BSA Curve.....	50
Figure 3.2 2D-Gel Image (Control).....	54
Figure 3.3 2D-Gel Images (7cm Controls).....	56
Figure 3.4 2D-Gel Images (7cm Experimental).....	58
Figure 3.5 2D-Gel Images (17cm Controls).....	60
Figure 3.6 2D-Gel Images (17cm Experimental).....	62
Figure 3.7 PDQuest Analysis-T0h Control MatchSet.....	67
Figure 3.8 PDQuest Analysis-T4h Control MatchSet.....	69
Figure 3.9 PDQuest Analysis-T24h Control MatchSet.....	71
Figure 3.10 PDQuest Analysis-Te4h Experimental MatchSet.....	73
Figure 3.11 PDQuest Analysis-Te24h Experimental MatchSet.....	75
Figure 3.12 Higher Level MatchSet-T0h and Te4h Comparison.....	77
Figure 3.13 Higher Level MatchSet-T0h and Te4h Comparison (enlarged view).....	79
Figure 3.14 Higher Level MatchSet-Unmatched Spots.....	81
Figure 3.15 Manual Comparison of T0h Control and Te4h Experimental MatchSet.....	83

List of Figures

Figure	Page
Figure 1.1 Myogenic Cells.....	9
Figure 1.2 Transcriptional Networks in Adult Myogenesis.....	11
Figure 1.3 Differentiating Myoblasts.....	13
Figure 1.4 Myogenic Differentiation Pathways.....	17
Figure 1.5 Components of the Cell-Cycle Control System.....	23
Figure 2.1 Two-Dimensional Gel Electrophoresis.....	39
Figure 3.1 Standard BSA Curve.....	50
Figure 3.2 2D-Gel Image (Control).....	54
Figure 3.3 2D-Gel Images (7cm Controls).....	56
Figure 3.4 2D-Gel Images (7cm Experimental).....	58
Figure 3.5 2D-Gel Images (17cm Controls).....	60
Figure 3.6 2D-Gel Images (17cm Experimental).....	62
Figure 3.7 PDQuest Analysis-T0h Control MatchSet.....	67
Figure 3.8 PDQuest Analysis-T4h Control MatchSet.....	69
Figure 3.9 PDQuest Analysis-T24h Control MatchSet.....	71
Figure 3.10 PDQuest Analysis-Te4h Experimental MatchSet.....	73
Figure 3.11 PDQuest Analysis-Te24h Experimental MatchSet.....	75
Figure 3.12 Higher Level MatchSet-T0h and Te4h Comparison.....	77
Figure 3.13 Higher Level MatchSet-T0h and Te4h Comparison (enlarged view).....	79
Figure 3.14 Higher Level MatchSet-Unmatched Spots.....	81
Figure 3.15 Manual Comparison of T0h Control and Te4h Experimental MatchSet.....	83

Stem Cells

In recent years, heightened interest in the therapeutic applications of cells possessing the ability to differentiate into a variety of cell types of multiple tissue lineages has developed. Scientists have focused on such stem cell research in the laboratory to investigate the underlying properties of self-renewal and lineage specification to aid in the advancement of damaged cell and tissue-based reparative therapies for diseases lacking effective treatments. Stem cell replacement and regenerative therapies potentially provide the basis for treatment of injury resulting from diseases including muscular dystrophy, multiple sclerosis, Parkinson's disease, Alzheimer's disease, heart disease, diabetes, and arthritis. Carefully, proteomic-based analysis in combination with genomic-based analysis may offer a more thorough understanding of the mechanisms of self-renewal and differentiation achieved by manipulation of stem cells *in vitro*, required for the clinical use of stem cells (Loebel et al., 2003; Tams et al., 2004).

CHAPTER I:

INTRODUCTION

What are the defining characteristics of stem cells? Stem cells are a population of infinitely dividing, self-renewing, undifferentiated cells that have the ability to produce a progeny of daughter cells with similar or opposite fates. Cell fate refers to the cell type a specific cell is most likely to give rise to during the normal developmental stages of the embryo. Through two strategies known as asymmetric asymmetry and divisional asymmetry, the homeostatic state of stem cells yields a generation of daughter cells containing 50% stem cells. For example, one of the daughter cells may retain the undifferentiated state of the parent stem cell, while the other acquires properties ultimately leading to terminal cell differentiation. Conversely, 100% of the daughter cells may retain

Stem Cells:

In recent years, heightened interest in the therapeutic applications of cells possessing the ability to differentiate into a variety of cell types of multiple tissue lineages has developed. Scientists have focused on such stem cell research in the laboratory to investigate the underlying properties of self-renewal and lineage specification to aid in the advancement of damaged cell and tissue-based reparative therapies for diseases lacking effective treatments. Stem cell replacement and regenerative therapies potentially provide the basis for treatment of injury resulting from diseases including muscular dystrophy, multiple sclerosis, Parkinson's disease, Alzheimer's disease, heart disease, diabetes, and arthritis. Currently, proteomic-based analysis in combination with genomic-based analysis may offer a more thorough understanding of the mechanisms of self-renewal and differentiation achieved by manipulation of stem cells *in vitro*, required for the clinical use of stem cells (Loebel *et al.*, 2003; Tannu *et al.*, 2004).

What are the defining characteristics of stem cells? Stem cells are a population of infinitely dividing, self-renewing, undifferentiated cells that have the ability to produce a progeny of daughter cells with similar or opposite fates. Cell fate refers to the cell type a specific cell is most likely to give rise to during the normal developmental stages of the embryo. Through two strategies known as environmental asymmetry and divisional asymmetry, the homeostatic state of stem cells yields a generation of daughter cells containing 50% stem cells. For example, one of the daughter cells may retain the undifferentiated state of the parent stem cell, while one inherits properties ultimately leading to terminal cell differentiation. Conversely, two similar daughter cells may retain

the same original fate and vary only in environmental cues causing terminal cell differentiation. The process of terminal cell differentiation entails a precursor cell's attainment of specialized tissue characteristics, regulated by external and internal cellular signals (Alberts *et al.*, 2002).

The two major types of stem cells, referred to as embryonic stem cells (ES) and adult stem cells, differ according to their developmental potential. Both types offer an opportunity for a thorough systemic analysis of the process of differentiation. *In vivo*, embryonic stem cells (ES) are a versatile source of totipotent precursor cells capable of producing every cell type in the embryo, while ES cultured *in vitro* are restricted to differentiation of many but not all cell types including hematopoietic, cardiac, and muscle. Embryonic stem cells are derived from the inner cell mass of preimplantation murine embryos and when supplemented with the appropriate culture factors can be manipulated to divide indefinitely, absent of terminal cell differentiation (Dinsmore *et al.*, 1996). By supplementation of the ES with combinations of growth factors to simulate the conditions of an *in vivo* environment, it has been possible to create nearly homogeneous populations of differentiated stem cells capable of producing functional derivatives. Studies have demonstrated improved behaviors of mice that "phenocopy" Parkinson's disease upon receipt of a successful engraftment of differentiated dopamine-producing neurons. Extensive experimentation with differentiated ES is necessary for the advancement of human stem cell therapies (Loebel *et al.*, 2003).

The second major type of stem cells, adult stem cells, primarily functions in the processes of regeneration and repair of cells of the same tissue type (Roelen and Dijke, 2003). Isolated from the bone marrow and periosteum of adult human and murine tissues,

multipotent stem cells termed “mesenchymal stem cells” possess the ability to differentiate into various mesenchymal cell lineages such as myoblasts, osteoblasts, and chondrocytes (Kadiyala *et al.*, 1997). Hormone-like proteins of the transforming growth factor- β (TGF β) superfamily, including TGF β s, bone morphogenetic proteins (BMPs), growth and differentiation factors (GDFs) and activins play an essential role in guiding mesenchymal cells to specific cell fate choices (Roelen and Dijke, 2003). Determined myoblasts, known as muscle precursor cells, develop into mature muscle fibers through the process of skeletal myogenesis (Amack and Mahadevan, 2004) (Figure 1.1).

Previous researchers have examined the effects of various agents on the process of muscular development. Agents including anabolic compounds such as testosterone and estradiol, synthetic analogues of glucocorticoids such as dexamethasone, growth factors like hepatocyte growth factor (HGF), and antioxidants such as quercetin and dimethylsulfoxide (DMSO) have been observed to effect the rates of myoblast proliferation and differentiation upon addition to myogenic cultures (Desler *et al.*, 1996; Gal-Levi *et al.*, 1998; Orzechowski *et al.*, 2001; Yang and Goldspink, 2002). Studies have identified the effects of testosterone on the development of different muscles, including development of the rat levator ani muscle at two critical time periods. Joubert *et al.*'s studies demonstrated that upon injection of testosterone during perinatal development, testosterone caused permanent changes in the levator ani muscle by increasing the rate of myoblast proliferation and/or the alignment and fusion of myotubes. The mechanism of testosterone released during puberty demonstrated increased proliferation of satellite cells to elevate the amount of myonuclei, most likely due to protein anabolism (Joubert *et al.*, 1993). There is also well-documented literature

confirming the enhanced protein synthesis and resulting increased muscle mass and strength following the administration of the androgen, testosterone (Mudali and Dobs, 2004). Also to be considered are the steroid hormone receptors, including the androgen receptor (AR) family that act in combination with steroid hormones and are known to influence development, differentiation, and homeostasis (Muller *et al.*, 2000). Although it is certain that the administration of testosterone exerts anabolic effects on proteins that ultimately increase skeletal muscle mass, the mechanism by which this occurs has not yet been determined. Clearly, advanced experimentation with both murine embryonic and adult tissue-derived cells will offer insight into essential strategies for human tissue growth, repair and replacement, and the means for a better understanding of the complex molecular mechanisms of proliferation and differentiation.

Myogenesis and Differentiation:

Myogenesis has been defined as a tightly-regulated, developmental program that controls the differentiation process of myoblasts (muscle precursor cells) into mature, muscle fibers (Amack and Mahadevan, 2004). The system provides a means of examining the molecular mechanisms underlying the cellular switch from proliferation to differentiation. Myogenesis is therefore recognized as an essential process in the generation of skeletal muscle in the embryo and the replacement skeletal muscle in the adult. Embryonically, the process of myogenesis occurs with the migration of muscle-cell precursors from the somites into specific sites of colonization, in which gene-regulatory proteins are expressed, followed by terminal differentiation (Buffinger and Stockdale, 1995).

Upon stimulation by various factors, the muscle precursor cells said to be “determined” to the myogenic cell type termed myoblasts, concomitantly express differentiation-specific genes and irreversibly withdraw from the cell cycle (Amack and Mahadevan 2004; Berry *et al.*, 2001; Gal-Levi *et al.*, 1998). Myoblasts continue to express myoblast-specific gene regulatory proteins belonging to the MyoD family of muscle regulating factors (MRFs,) encoded by the *myoD* gene, and MEF2 regulatory proteins encoded by the *MEF2* gene. The MRFs are a group of helix-loop-helix transcription factors (HLH-TFs) including MyoD, myf5, MRF4, and myogenin. MyoD and myf5 expression are associated with the myogenic lineage determination, while MRF4 and myogenin are involved in myogenic differentiation (Berry *et al.*, 2001; Shen *et al.*, 2003) (Figure 1.2). These muscle regulatory factors “form heterotrimers with ubiquitous bHLH nuclear proteins (E proteins) and act in cooperation with the MEF2 family members, thereby binding E boxes (MEF1) and MEF2 sites on muscle-specific gene promoters and activating these genes” (Gal-Levi *et al.*, 1998). MEF2 members can only initiate the myogenic activities of MRFs when associated with MRFs (Shen *et al.*, 2002).

Based on the plasticity of immature cell types, overexpression of MRFs have the capability of forcing the conversion of non-muscle cells into myogenic cells, such as chondrocytes into cells of the myogenic cell lineage (Buffinger and Stockdale, 1995). Such plasticity was evident when bone morphogenetic protein-2 (BMP2), regulated by a myogenic HLH-TF, induced bone formation following implantation into muscle tissue (Liu *et al.*, 1997). Okubo *et al.* also demonstrated the arrest of terminal cell differentiation in C2C12 myoblasts and the conversion of such cells to the osteogenic

lineage upon addition of BMP-2 to culture medium (Okubu *et al.*, 1999). Enhanced expression of MyoD in non-muscle cells forced these cells to the myogenic lineage, causing muscle-specific genes to be activated (Berry *et al.*, 2001).

The aspect of myogenesis named “myoblast differentiation” refers to the period following proliferation in which the myoblast overtly switches to a more specialized cell type. Through cellular membrane fusion, mononucleated myoblasts align to form multinucleated myotubes and are ultimately organized into mature myofibers with contractile ability (Amack and Mahadevan, 2004; Kim *et al.*, 1999; Orzechowski *et al.*, 2001) (Figure 1.3a and 1.3b). The efficiency of the fusion process is enhanced by a phenomenon known as the “community effect” which directs identical, adjacent groups of myoblasts to complete the process of differentiation (Kim *et al.*, 1999). At the point of terminal differentiation when mature myotubes are formed, cell division is terminated. Upon damage to mature myotubes, mononucleated cells known as satellite cells, essential for growth, regeneration and repair, are recruited (Amack and Mahadevan, 2004).

Figure 1.1: Myogenic Cells

Chronological organization of cells involved in myogenesis, including satellite cells, myoblasts, myotubes, and mature, contractile muscle fibers.

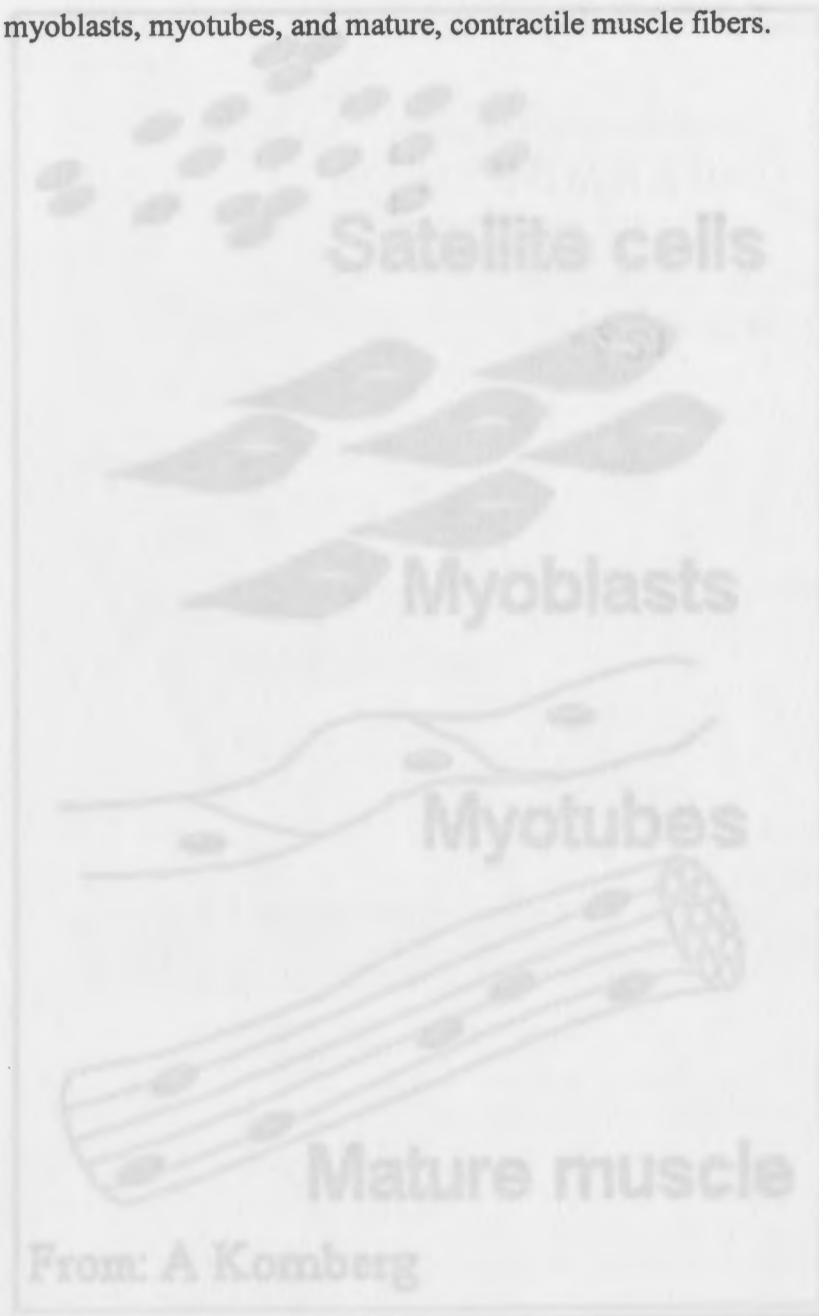


Figure 1.1 Looking Back to the Future

Defining Transcriptional Networks in Adult Myogenesis

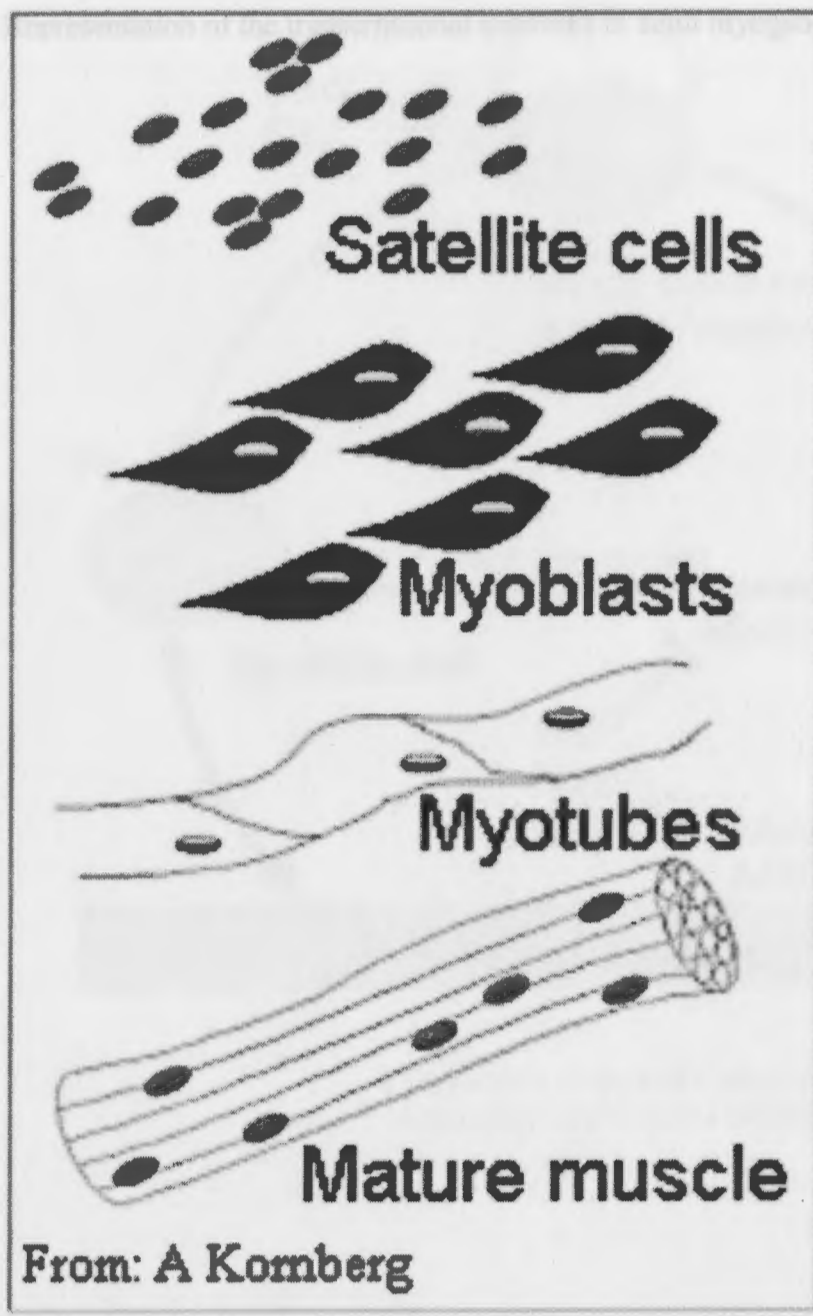


Figure 1.2: Looking Back to the Embryo:

Defining Transcriptional Networks in Adult Myogenesis

Representation of the transcriptional networks in adult myogenesis.

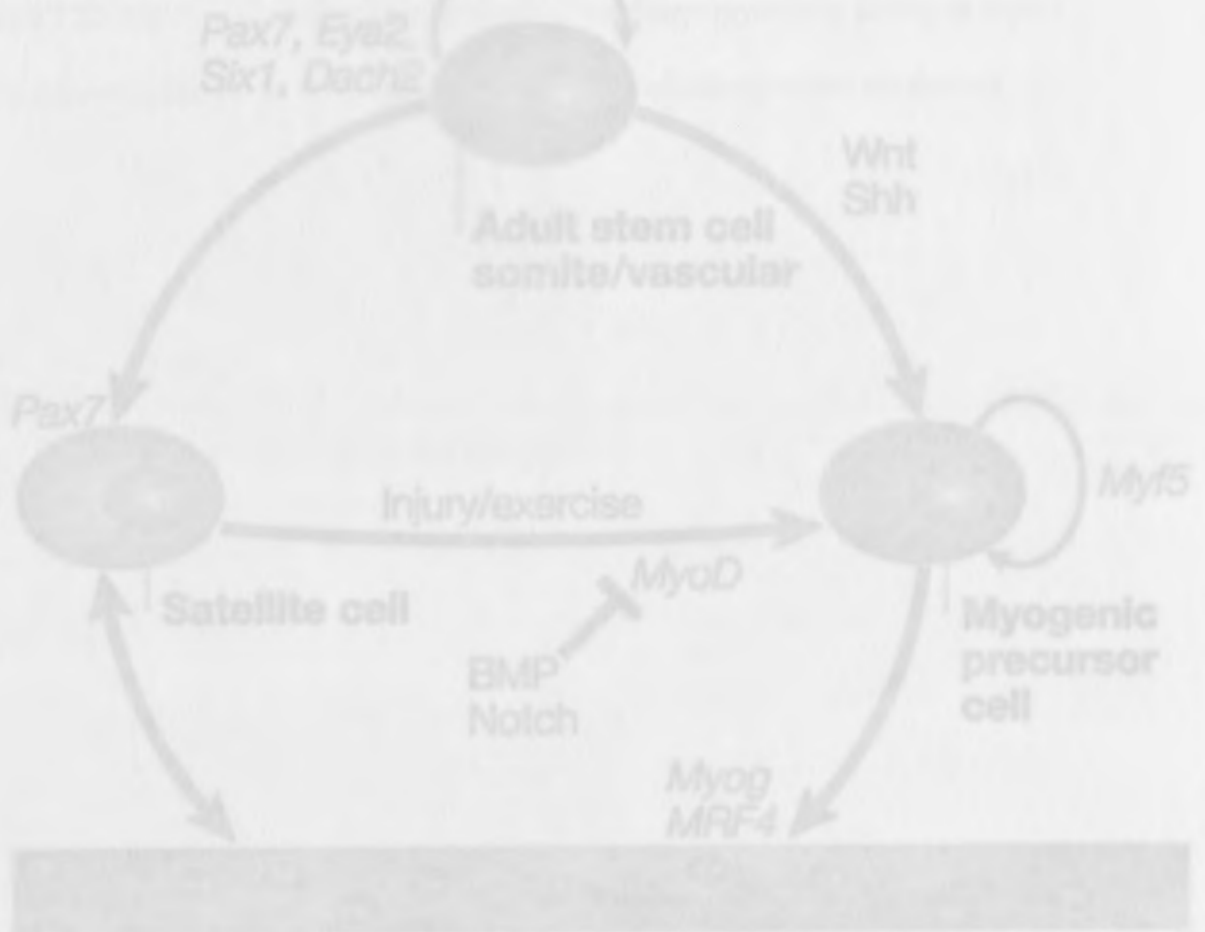
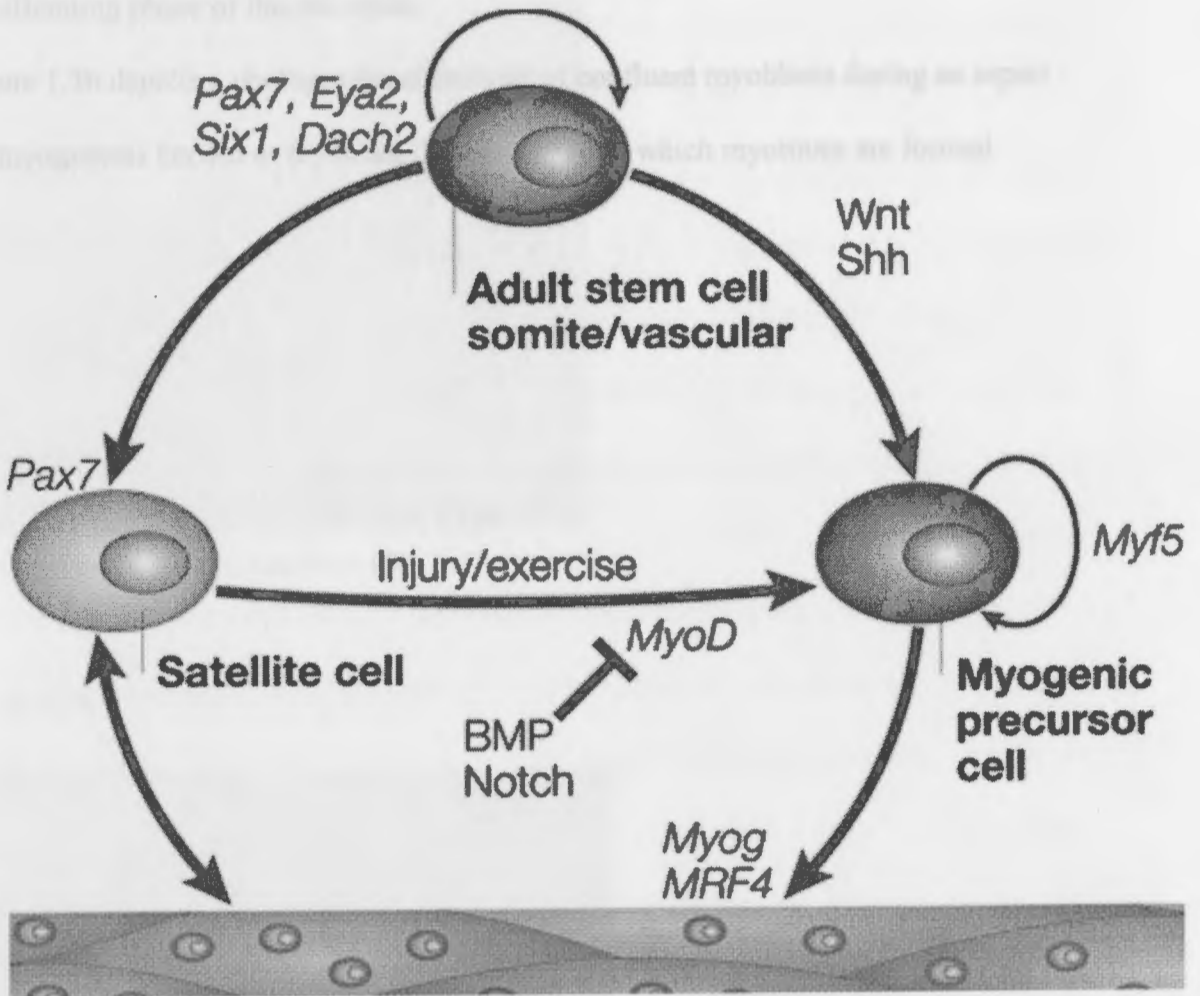


Figure 1.2

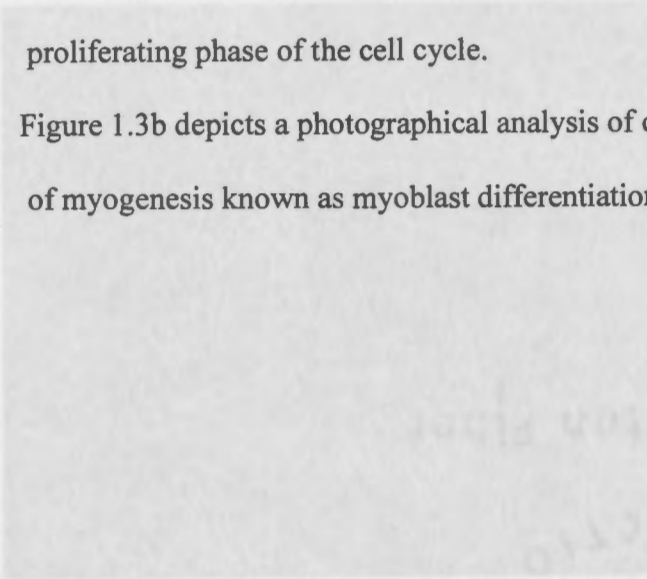


Components of the Cell Cycle Control System
(*Nature Reviews Genetics* (2003) 4: 497-507).

Figure 1.3: Proliferating and Differentiating Myoblasts

Figure 1.3a depicts a photographical analysis of subconfluent myoblasts during the proliferating phase of the cell cycle.

Figure 1.3b depicts a photographical analysis of confluent myoblasts during an aspect of myogenesis known as myoblast differentiation in which myotubes are formed.



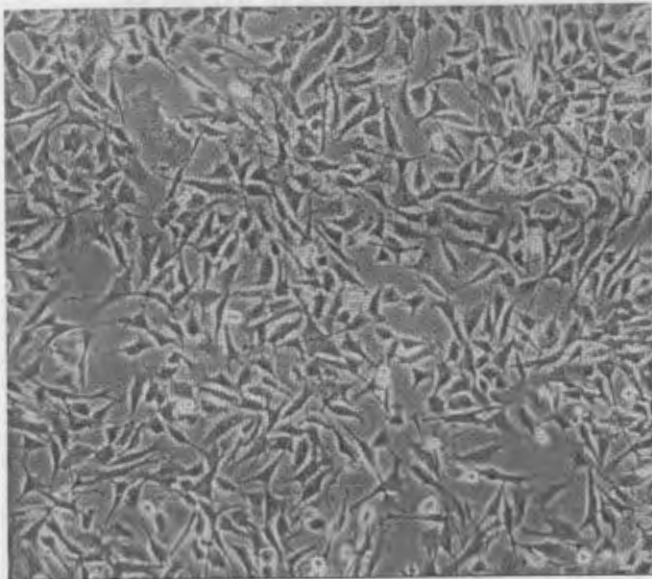
www.nandachweb.org/articles/news/2/3/12/1/180803

Figure 1.3b



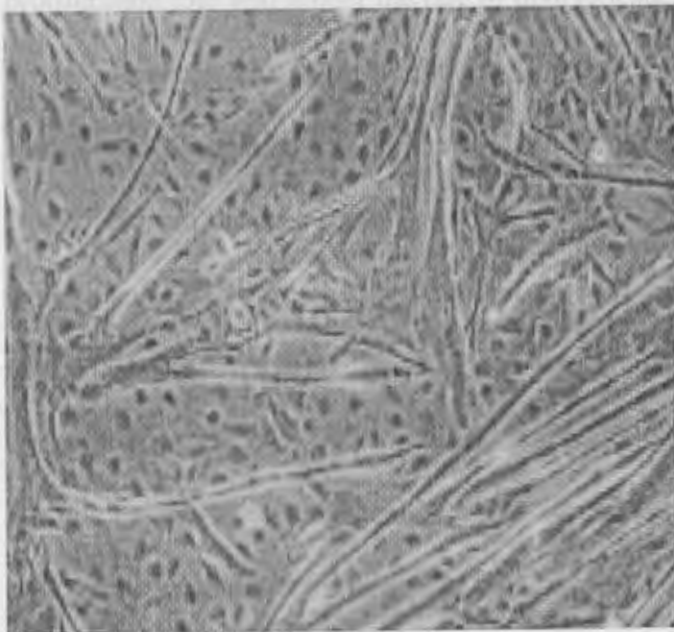
Molecular Biology Reports 27: 87-96, 2020

Figure 1.3a



www.nanotechweb.org/articles/news/2/8/12/1/180803

Figure 1.3b



Molecular Biology Reports 27:87-88, 2000

Muscle Growth and Regeneration:

The growth and regeneration of skeletal muscle cells is largely dependent upon nearby cells uniformly located within the basal lamina of myofibers. The inactive cells named satellite cells remain in close proximity to the mature muscle cells for emergency purposes. Upon injury to neighboring muscle tissues, satellite cells inherently proliferate and fuse with one another while simultaneously expressing muscle-specific proteins (Figure 1.4). The majority of extracellular activators and inhibitors of satellite cell proliferation and differentiation remain undefined, while growth factors such as insulin-like growth factors I and II (IGF-1 and IGF II), transforming growth factor beta (TGF- β), and growth hormone have been implicated (Gal-Levi *et al.*, 1998).

Although the mechanisms of satellite cell recruitment for regeneration or hypertrophic purposes remains elusive, it has been suggested that an increased proliferation rate will hinder the rate of myogenesis and therefore increase the mass of the growing muscle. The mitogenic antioxidant, quercetin, has been identified as a possible contributor to increased muscle mass, due to delayed myogenesis and the presence of less numerous, but larger myotubes after C2C12 myoblast treatment. Conversely, the antioxidant DMSO markedly inhibited myogenesis, therefore proposing avoidance of DMSO during required periods of accelerated muscle growth and regeneration (Orzechowski *et al.*, 2001). Additional findings have suggested the influence of hepatocyte growth factor (HGF) and its receptor, c-met, on muscle satellite cell proliferation and differentiation inhibition (Gal-Levi *et al.*, 1998).

The population of satellite cells becomes useful in some forms of muscular dystrophy, including a type in which the myotubes are damaged because of defects in the

genetic conformation of the protein dystrophin, called Duchenne muscular dystrophy (DMD) (Noguchi *et al.*, 2003). Previous attempts at transplanting myoblasts into damaged tissues of mice to restore dystrophin function were only successful when mice were previously irradiated with damaging chemicals. However, pretreatment of mice with concanavalin A (ConA) did improve myoblast migration into transplanted tissues (Ito *et al.*, 1998). Studies have revealed in myotonic dystrophy type 1 (DM1), a mutant DM protein kinase (DMPK) contributes to an altered myogenic process causing smaller myofibers and increased satellite cell numbers (Amack and Mahadevan, 2003). A number of glucocorticoid drugs like dexamethasone, have been implicated to improve the damaging effects of DMD. Glucocorticoids reportedly increase the mRNA expression of satellite cell-proliferation genes (MRFs), which in turn activate satellite-cell specific genes that respond to injury of muscle fibers. Also, it has been suggested that glucocorticoid treatment decreases the differentiation of C2C12 myoblasts, indicated by decreased levels of myogenin mRNA (te Pas *et al.*, 2000). An increased differentiation rate of C2C12 myoblasts treated with dexamethasone compared to untreated C2C12 cells was observed in G.R.Walker's lab based on resulting increased myotube formation following dexamethasone treatment (Lariviere 2002).

When the satellite cells have exacerbated any further regeneration possibilities because of the heightened pace of damage, connective tissue replaces muscle tissue (Alberts *et al.*, 2002). Extended research concerning myoblast function and investigation of the specific proteins expressed in myogenic differentiation could formulate solutions to these exhausted satellite cell lines.

Figure 1.4: Myogenic Differentiation Pathways

Myogenic differentiation pathways of embryonic, regenerative, and C2C12 myoblasts.

A. Embryonic myogenesis



B. Regenerative myogenesis

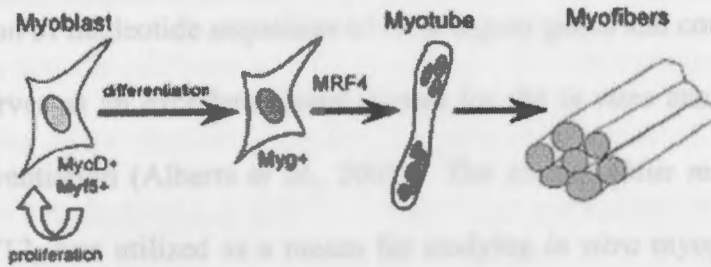


C. C2C12 myogenesis

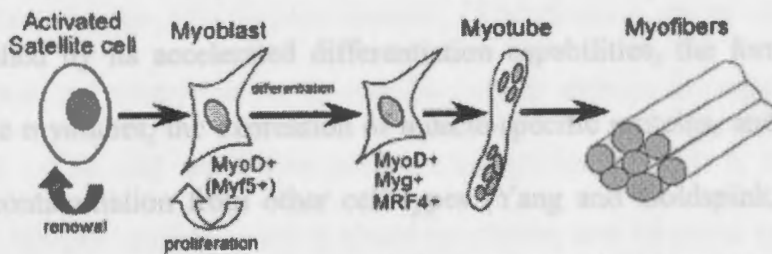


Figure 1.4

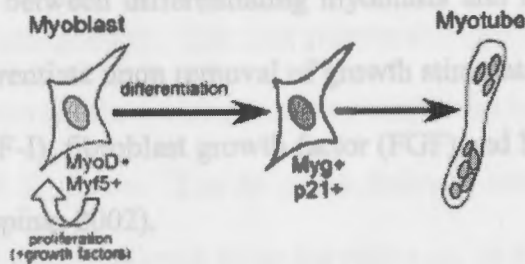
A. Embryonic myogenesis



B. Regenerative myogenesis



C. C2C12 myogenesis



J.D. Amack, M.S. Mahadevan / *Developmental Biology* 265 (2004) 294–301

C2C12 Cell Line:

Due to the close genetic resemblance of all mammalian species discovered by the comparison of nucleotide sequences of orthologous genes and corresponding proteins, the mouse serves as an excellent model system for the *in vitro* analysis of myogenesis and cell differentiation (Alberts *et al.*, 2002). The murine (*Mus musculus*) myoblastic cell line, C2C12, was utilized as a means for studying *in vitro* myogenic differentiation and cell cycle simultaneously with testosterone-effect analysis. The C2C12 line is distinguished by its accelerated differentiation capabilities, the formation of extensive contractile myotubes, the expression of muscle-specific proteins, and the ability to grow without contamination from other cell types (Yang and Goldspink, 2002). Fusion of cellular membranes requires cell-cell adhesion molecules necessary for recognition occurring between differentiating myoblasts and muscle fibers (Kim *et al.*, 1999). The cells differentiate upon removal of growth stimulatory factors such as insulin-like growth factor (IGF-I), fibroblast growth factor (FGF) and hepatocyte growth factor (HGF) (Yang and Goldspink, 2002).

Previous studies suggest the existence of a specific time parameter in which fusion occurs, while “spaciotemporal coordination” guarantees homogenous myotube cultures. Mature skeletal muscle cells are the result of these cell-cell adhesions. Furthermore, expression of specific myogenic proteins stimulates the transcription of other muscle-regulatory genes, resulting in an amplified feedback system for continuation of muscle development (Kim *et al.*, 1999).

Cell Cycle Control:

The C2C12 line has been utilized as an *in vitro* model for studying cell cycle withdrawal associated with cellular differentiation. The arrest of the cell-division cycle is crucial to muscle differentiation. Under specific environmental conditions, actively proliferating cells, including myoblasts, undergo a series of events causing cellular growth for protein synthesis and DNA replication, and cellular division, in which one cell produces two daughter cells.

What is the cell-division cycle? Cell-division cycle refers to the timed mechanisms in eukaryotic organisms by which mitosis is regulated and DNA is replicated. The cell replication program progresses through a sequence of phases, including the two major phases, S phase (synthesis) and M phase (mitosis). Following genomic DNA duplication in the S phase, the G₂ or gap phase occurs to allow for extended cell growth. The gap phases also provide ample time for the cell to ensure proper environmental and preparatory conditions before entering the dramatic phases of S phase and M phase. The M phase follows, inducing a cascade of events leading to nuclear division, referred to as karyokinesis, in which the cell containing two pairs of sister chromatids separate into two separate chromosomes and reform intact nuclei. Cell division is complete when cytoplasmic division, or cytokinesis, causes the separation of the cell into two daughter cells. The newly formed separate entities will then enter into the G₁ phase, enhancing the growth of the cell. The cycle is then reinitiated (Lodish *et al.*, 2000).

The cell-cycle control system exerts ultimate control over the various mechanisms of the cell-division cycle by producing both stimulatory and inhibitory intracellular

signals, and specific checkpoints for completion of the phases (Figure 1.5). The two most important families involved in the cell-cycle control system are the heterodimeric protein kinases, cyclins and cyclin-dependent kinases (Cdks). The cyclin associated with the Cdk subunit will modulate which proteins the Cdk-cyclin complex will phosphorylate (Lodish *et al.*, 2000; Kitzmann and Fernandez, 2001). Inactivation/activation of such complexes induces fluctuations in the phosphorylation of amino acid residues, for example, which regulate the phases of the cell-division cycle. Cell division cycle 2 (*cdc2*) is a cyclin-dependent kinase known to be a 34kD protein called $p34^{cdc2}$, which controls the cell's entry into M phase (Wada *et al.*, 2004). Other proteins such as gene regulatory protein p53, inhibits cells from proceeding through both gap phases when damaged DNA is present (Lodish *et al.*, 2000).

Because many of the underlying cellular mechanisms that modulate cell cycle and division are unknown, indefinitely growing cells of *in vitro* culture remain an infinite source of knowledge to cell biologists and molecular geneticists. Studies have implicated an MRF protein, MyoD, for its role in the arrest of the cell cycle by the induction of p21, a cyclin-dependent kinase inhibitor and the induction of retinoblastoma protein (Shen *et al.*, 2002). Another marker of muscle differentiation, Bcl-2, is an "antiapoptotic protein that is phosphorylated and inactivated by Cdk2 kinase during G2/M transition in proliferating cells, was dephosphorylated and, hence, activated during C2C12 cell differentiation" (Shen *et al.*, 2003). Additionally, the expression of the G1 regulatory protein, $p21^{WAF/Cip1}$, functioned to maintain cell-division cycle in muscle cells (Shen *et al.*, 2003).

Studies have also identified the mammalian target of the immunosuppressant rapamycin, mTOR, for its role in regulating various components of the “translational machinery” of the cell (Proud 2003). A kinase domain related to the phosphatidylinositol kinase-related kinase family known to regulate cell cycle, is located near mTOR’s C-termini. Rapamycin interferes with the G1-phase progression and cellular signalling by inhibiting the function of the protein mTOR, which is essential to the process of skeletal muscle differentiation (Brunn *et al.*, 1997). Upon treatment of C2C12 myoblasts with the prokaryotic nucleoside N⁶-Methyldeoxy-adenosine (MedAdo), a marked increase in the expression of regulatory proteins p21^{WAF/Cip1}, myosin heavy chain protein, and mTOR were detected. Thus, MedAdo forced the cells towards the myogenic lineage pathway (Charles *et al.*, 2004). Because mTOR signaling occurs by amino acid and hormone stimulation, such as insulin, many questions remain to be answered. For example, is mTOR signaling activated by the administration of the steroid hormone testosterone? Also, how does mTOR force C2C12 myoblasts into the myogenic lineage? Additional findings may pinpoint the phosphorylation of various cell-division cycle proteins involved in myogenic differentiation pathway upon treatment with the testosterone.

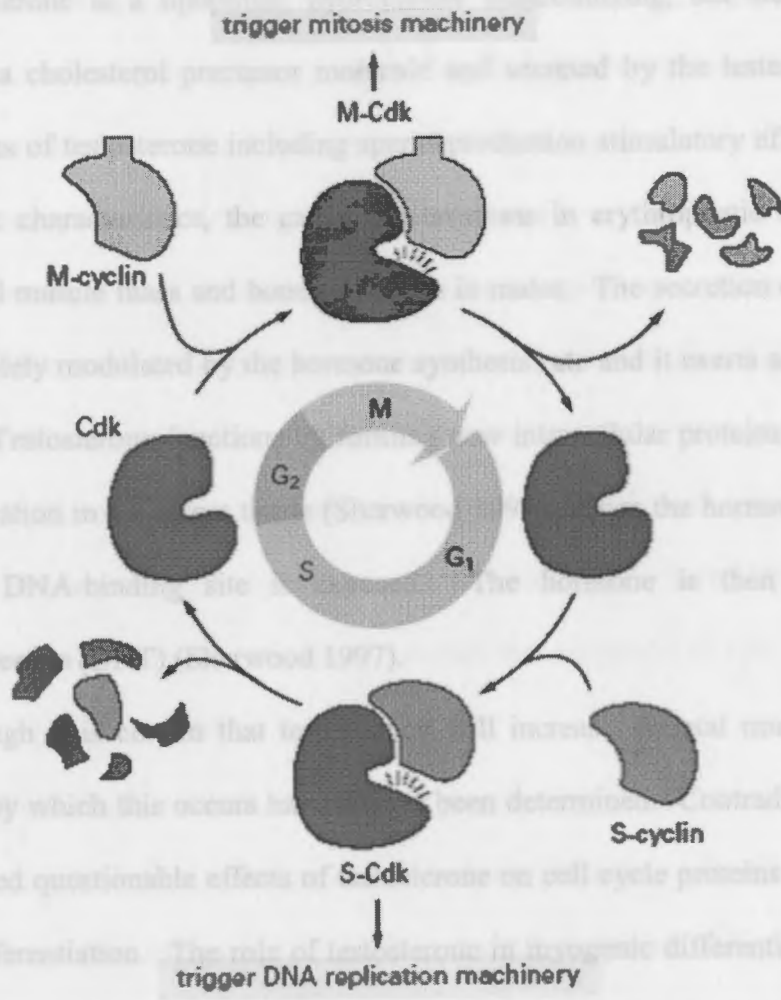
Figure 1.5: Components of the Cell-Cycle Control System

Components involved in the progression of the cell through the phases of cell-division cycle.



Molecular Biology of the Cell

Figure 1.5



Molecular Biology of the Cell

Effects of Testosterone:

Testosterone is a lipophilic, hydrophobic masculinizing, sex steroid hormone derived from a cholesterol precursor molecule and secreted by the testes. There are many functions of testosterone including sperm production stimulatory effects, a role in secondary sex characteristics, the cause of elevations in erythropoietic basal rate and higher skeletal muscle mass and bone formation in males. The secretion of testosterone secretion is solely modulated by the hormone synthesis rate and it exerts anabolic effects on proteins. Testosterone functions by forming new intracellular proteins, as a result of the gene activation in the target tissue (Sherwood 1997). Once the hormone binds to its receptor, its DNA-binding site is exposed. The hormone is then converted to dihydrotestosterone (DHT) (Sherwood 1997).

Although it is certain that testosterone will increase skeletal muscle mass, the mechanisms by which this occurs have not yet been determined. Contradictory findings have implicated questionable effects of testosterone on cell cycle proteins and its role in myogenic differentiation. The role of testosterone in myogenic differentiation has been examined, revealing DHT and testosterone control lineage determination in mesenchymal stem cells by forcing them into the myogenic lineage (Singh *et al.*, 2003). The effects of testosterone were analyzed in the levator ani muscle of the rat. Although the levator ani is present in both males and female rats at birth, it atrophies in the female. When female rats were treated with testosterone at birth, there was a marked mass increase in the levator ani muscles (Albis *et al.*, 1992). Additional studies focusing on the treatment of sarcopenia, a form of muscle loss prevalent among the elderly, have identified a genetically altered skeletal muscle cell line, the C2C12 line, that responded to

hypertrophy-inducing agents. Hypertrophy refers to the enlargement of a tissue due to increased cell size. The C2C12 line, altered by the addition of the β -myosin heavy chain gene promoter and enhancer regions, responded to hypertrophy-inducing agents like testosterone and insulin. Such a hypertrophy-responsive system could offer insight into unknown hypertrophy-induction signals. (Cross-Doerson and Isfort, 2003). Studies involving testosterone have shown that the testosterone was not a causal factor in the difference between male and female myosin transition from embryonic to adult isoforms (Albis *et al.*, 1992). Some studies suggest that *in vitro* cultures of rat myogenic cell lines treated with testosterone cause a decrease in cell cycle time and the G₁ phase, while other studies show that testosterone does not elevate myoblast production (Skjaerlund *et al.*, 1994). Dihydrotestosterone was shown to increase the activation of p38, a sex-specific MAP kinase (Angele *et al.*, 2003).

The effects of testosterone on the underlying mechanisms of muscle development and cell cycle require further investigation. This study proposes to examine the effect of testosterone on protein expression in C2C12 myoblasts during differentiation. The approach taken is a proteomic approach.

Proteomics:

Proteomics is a novel technique based on the qualitative and quantitative analysis of the proteome, or the full set of proteins expressed by the genetic material of an organism. Proteomics serves to complement information achieved by the analysis of the transcriptome alone, through the achievement of the functions of proteins during varying cellular conditions (Graves and Haystead, 2002). Proteomic-based analysis involves two

revolutionary techniques including two-dimensional gel electrophoresis (2DGE) in combination with mass spectrometry. Such analyses allows for the quantitation and identification of specific peptides in a complex protein mixture, including whole cell lysates. Proteomic-based analysis offers insight into the unknown cellular processes, like proliferation and differentiation, due to the creation of protein maps visualized by polyacrylamide gels and highly sensitive staining. As a result of such protein maps, information pertaining to the upregulation and downregulation of proteins, changes in protein isoforms, and post-translational modifications can be achieved. Upon further computer-based analyses and mass spectrometry, proteins involved in varying cellular conditions may be identified (Görg *et al.*, 2004).

Goals of Proposed Study:

The aim of this study was to offer a comparative, combinatorial analyses of the total proteome, upon differentiation of C2C12 myoblasts at zero, four and twenty-four hours after induction of differentiation, with or without testosterone treatment. Protein maps at each time point are then compared to each other and changes in protein composition can then be used to identify potentially important proteins. Proteins identified in this way will yield insight into the unknown cellular mechanisms involved in the effects of testosterone on C2C12 myoblast differentiation, to ultimately aid in the battle against muscular disease. We hypothesized the identification of differential protein expression at each time point, linked to changes in gene expression during differentiation of testosterone-treated and untreated C2C12 myoblasts.

Experimental Approach to C2C12 Differentiation

The C2C12 cell culture system was utilized to examine the factors regulating muscle development through the processes of proliferation and differentiation. Upon administration of the anabolic steroid testosterone to the appropriate growth media, treated samples were collected in a time-dependent manner starting at time 0h, 4h, and 24h following induction of differentiation. Testosterone samples from both treated and untreated cells were analyzed by comparative protein analysis using two-dimensional gel electrophoresis (2DGE) and ProQuest™ 2-D Analysis Software for the identification of the appearance and disappearance of regulatory proteins.

CHAPTER II:

MATERIALS AND METHODS

C2C12 Culture (Mus musculus)

The 3H strain of a C2C12 mouse myoblastic cell line purchased from ATCC were cultured in sterile, vented-cap culture flasks (75cm²) in 15mL of filter-sterilized growth medium under a laminar flow hood intermittently sterilized by ultraviolet light. C2C12 cells were cultured in pre-incubated (37° Celsius) growth medium to obtain proper pH. The growth medium consisted of Dulbecco's Modified Eagle's Medium (DMEM) (1000mg/L glucose, L-glutamine, sodium bicarbonate), 10% Fetal Bovine Serum (FBS), and penicillin-streptomycin (P-S) (10,000IU/ml and 10,000 µg/ml) in which the cells were incubated at 37°C in 5% CO₂. Using appropriate ventilation techniques, growth medium was renewed every two days. To monitor factors including cell density, cell removal, and morphological characteristics such as myotube formation, cells were observed daily under an Olympus TG41 microscope linked to a monitor.

Experimental Approach to C2C12 Myogenesis:

The C2C12 cell culture system was utilized to examine the factors regulating muscle development through the processes of proliferation and differentiation. Upon administration of the anabolic steroid testosterone to the appropriate growth media, treated samples were collected in a time-dependent manner starting at time 0h, 4h, and 24h following induction of differentiation. Triplicate samples from both treated and untreated cells were analyzed by comparative protein analysis using two-dimensional gel electrophoresis (2DGE) and PDQuest™ 2-D Analysis Software for the identification of the appearance and disappearance of regulatory proteins.

C2C12 Culture (*Mus musculus*):

The 3H strain of a C2C12 mouse myoblastic cell line purchased from ATCC were cultured in sterile, vented-cap culture flasks (75cm²) in 15mL of filter-sterilized growth medium under a laminar flow hood intermittently sterilized by ultraviolet light. C2C12 cells were cultured in pre-incubated (37° Celsius) growth medium to obtain proper pH. The growth medium consisted of Dulbecco's Modified Eagle's Medium (DMEM) (1000mg/L glucose, L-glutamine, sodium bicarbonate), 10% Fetal Bovine Serum (FBS), and penicillin-streptomycin (P-S) (10,000IU/ml and 10,000 µg/ml) in which the cells were incubated at 37°C in 5% CO₂. Using appropriate sterilization techniques, growth medium was renewed every two days. To monitor factors including cell density, cell removal, and morphological characteristics such as myotube formation, cells were observed daily under an Olympus T041 microscope linked to a monitor.

The C2C12 cells were sub-cultured by rinsing gently with 5ml of 0.25% (w/v) Trypsin-0.53mM EDTA solution to ensure removal of serum that may inhibit trypsin effectiveness. Cells were then eluted with 7ml of 0.25% (w/v) Trypsin-0.53mM EDTA solution upon 70-80% confluency, incubated for approximately 20 minutes, transferred to new culture flasks, and resuspended in 15ml of pre-incubated 10% FBS/DMEM/P-S. To harvest C2C12 cells, cells were rinsed gently with 5ml of 0.25% (w/v) Trypsin-0.53mM EDTA solution and eluted with 7ml of 0.25% (w/v) Trypsin-0.53mM EDTA solution. After an incubation time of 20 minutes in which the cells had visibly detached from plastic surface, cells were vortexed and washed 3X with 10ml of 1X Trans Buffered Saline (TBS) by centrifugation at 2000 rpm for five minutes per wash. Upon removal of TBS, pelleted cells were stored in a -80° Celsius freezer for later use. Cells required for additional cultures were harvested at 70-80% confluency (according to described harvesting procedures) with the addition of a 5% (v/v) dimethylsulfoxide (DMSO) solution to pelleted cells, frozen in the -80° Celsius freezer for 60 minutes, then transferred to a liquid nitrogen storage tank.

Growth medium was reduced to a 1% FBS/DMEM/P-S solution to induce differentiation of C2C12 myoblasts. Alternatively, differentiation medium supplemented with a 1 μ M testosterone/ethanol solution was administered for comparison of both treated and untreated cells. Treated (experimental) and untreated (control) cells were harvested at 0h, 4h, and 24h following induction of differentiation and subjected to further analysis by two-dimensional gel electrophoresis and PDQuest Analysis.

C2C12 culture aids in the detection of various proteins of interest expressed at different stages of cell cycle. Triplicate samples were collected for the mapping of pre

and post-differentiation proteins. Proteins were analyzed upon treatment of C2C12 cells with growth media containing testosterone, before and after differentiation. Alterations in patterns, time course differences, clarifications of molecular processes, and functional differences may be determined from excised proteins.

Protein Preparation and Quantitative Protein Analysis:

Pelleted C2C12 cells (1 pellet/culture flask) were diluted with 500ml of Sample Buffer (low-active rehydration buffer) containing 8M urea, 2% CHAPS, and 50mM dithiothreitol (DTT). Suspended cells were sonicated with the Cell Disrupter 3X at 15 seconds per sonication on ice followed by a 60 second delay between sonications. Lysed cells were microcentrifuged at 2000 rpm for five minutes per centrifugation and the supernatant was recovered.

To quantify the amount of protein in solution, samples were subjected to a modified Bradford Assay. The modified Bradford Assay, a technique slightly modified from the original Bradford Assay, is a fast and accurate method for the determination of total protein concentration of a sample. Protein concentrations (μg) were determined by the absorbance of the protein-dye binding complex at 595nanometers (nm) in comparison to a bovine serum albumin (BSA) standard (Bradford, 1976). The Modified Bradford Assay required a Coomassie brilliant blue dye known to specifically bind proteins primarily at arginine residues. The shift in absorbance of the protein-dye binding complex was measured by a spectrophotometer (Hewlett-Packard 8453 UV-Visible System). A standard concentration curve representing a linear relationship between protein-dye binding, depicted by known amounts of protein per unit volume ($\mu\text{g}/\mu\text{L}$), versus the change in absorbancy at 595nm (Optic Density) was constructed. The

standard concentration curve was used to convert the unknown amount of O.D. to the actual concentration, by using the equation that fits the curve. The resulting R^2 value must be 0.95 or higher. If the extinction coefficient was higher than 1, the sample must be diluted and factored into the equation.

The Modified Bradford Assay procedures included preparing standards containing 10, 15, 20, 25, 30, 35, and 40 microgram (μg) quantities of BSA. To each test tube, 80 μL of Deionized (DI) H_2O , 10 μL of 0.1M Hydrochloric acid (HCl), 10 μL of two-dimensional electrophoresis (2-DE) buffer (8.4 M urea, 2.4 M thiourea, 5% CHAPS, 25 mM spermine base, 50 mM dithiothreitol) and 4mL of Bradford dye were added. A blank was prepared by adding 4 ml of Bradford dye to an individual test tube. To separate test tubes, the unknown sample concentrations of harvested C2C12 cells were determined by adding 10 μL of sample previously suspended in Sample Buffer, 80 μL of DI H_2O , 10 μL of 0.1M HCl, 10 μL of 2-DE buffer (8.4 M urea, 2.4 M thiourea, 5% CHAPS, 25 mM spermine base, 50 mM dithiothreitol) and 4mL of Bradford dye. After a five-minute setting period, and a 15-minute warming period for the spectrophotometer, the solutions were transferred to plastic cuvettes. Following the blanking procedure, the absorbances of the standard and unknown samples were measured using UV-Visible light at 595 nm.

Analysis by two-dimensional gel electrophoresis (2DGE):

Two-dimensional gel electrophoresis results in the separation of proteins based on differences in charge and mass. Firstly, isoelectric focusing (IEF) separates proteins by differences in isoelectric pH (pI in which the net charges are zero). Secondly, sodium dodecyl sulfate polyacrylamide gel electrophoresis (SDS-PAGE) separates proteins

through a porous acrylamide gel matrix by molecular mass (M_r) differences by a constant voltage using immobilized pH gradient (IPG) strips. This revolutionary technique allows for the identification of proteins in previously ambiguous molecular processes and complements information achieved by analysis of the transcriptome. From the visible protein “maps” created, pertinent information such as changes in protein expression and posttranslational modifications can be inferred. The detection of certain proteins may formulate insight into unknown cellular mechanisms of for example, disease-specific protein markers (Beranova-Giorgianni 2003; Candiano *et al.*, 2002; Cleveland *et al.*, 1977; Görg *et al.*, 2004; Tannu *et al.*, 2004) (Figure 2.1).

Active Rehydration and Isoelectric Focusing-

1st Dimension:

Upon completion of the Modified Bradford assay, the proper concentration of sample load was determined based upon 100 μ g of protein for 7cm immobilized pH gradient strips (IPG) and 400 μ g of protein for 17cm immobilized pH gradient strips (IPG). Ampholytes preformed into the gel strip establish the pH gradient in the gel, resulting in migration of the proteins to their isoelectric pH (pI). The preset pH gradient cast into the gel strip eliminates problems such as gradient drift. IPG strips from the 4-7 pH and 3-10 pH gradient ranges were utilized. The proper volume of sample, 125 μ l for 7cm IPG and 300 μ L for 17cm IPG strips, was loaded into a Bio-Rad PROTEAN[®] IEF focusing tray and the ReadyStrip[™] IPG strip (purchased from Bio-Rad) was placed gel-side down in the IEF focusing tray, while directly contacting the electrodes. Bubbles were removed by carefully lifting the strip up and down to eliminate interference with

isoelectric focusing. The strips were then overlaid with mineral oil to prevent dehydration, placed into the PROTEAN® IEF cell and programmed for rehydration under active conditions at 20° Celsius, 50 Volts for approximately 12 hours. A pause was inserted following rehydration to place H₂O-saturated wicks over the electrodes. Focusing conditions for 7cm strips were set linearly to 40000 volt-hours (V-hr) with a maximum current of 50µA per strip and a default temp of 20° Celsius. Focusing conditions for 17cm strips were set linearly to 60000 V-hr, with a maximum current of 50µA per strip and a default temp of 20° Celsius. The IPG strips were held at a 500V hold upon completion of rehydration and isoelectric focusing. The entire 1st dimension process required approximately 24 hours. Strips are either frozen for future analysis or subjected to SDS-PAGE.

Sodium dodecyl sulfate polyacrylamide gel electrophoresis (SDS-PAGE)-

2nd Dimension:

Upon completion of 1st dimension, a loading tray was prepared with 2.5-6.0mL of Equilibration buffer I (6M Urea, 0.375 M, pH 8.8, 2% SDS, 20% glycerol, 2% (w/v) DTT). Excess mineral oil was removed from the ReadyStrip™ IPG strips by carefully draining and blotting on moistened KIM wipes. The IPG strips were inserted gel-side up into the loading tray and shaken on an orbital shaker for 10 minutes on speed two. The IPG strips were then placed gel-side up into a loading tray containing 2.5-6.0mL of Equilibration buffer II (6M Urea, 0.375M Tris, pH 8.8, 2% SDS, 20% glycerol, and 2.5% (w/v) iodoacetamide) and were shaken for a minimum of 10 minutes. The addition of iodoacetamide alkylates free DTT and prevents reoxidation of sulfhydryl groups (Görg *et*

al., 2004). A loading tray was then filled with 4mL of 1x Tris-glycine-SDS (TGS) running buffer. Before applying the strip to the glass gel plate, an agarose overlay (5% agarose) was heated until fully liquefied and pipetted over the gel strip while simultaneously inserting the gel strip onto the glass gel plate. Both 10% and 12% polyacrylamide gels were made 24 hours prior to 2nd dimension procedures. (See Gel Components Table 2.1) Timing was essential as to not allow the agarose to solidify before the gel strip was inserted. Any excess air was removed, and adequate solidification time was necessary.

A 1X TGS buffer was filled to staggered levels inside and outside of the electrophoresis chambers, Bio-Rad's Mini-PROTEAN[®] 3 for 7cm strips and the PROTEAN II XL Electrophoresis chamber for 17cm strips. SDS is an anionic binding detergent resulting in overwhelmingly negative proteins. When current is applied, the proteins are forced to travel to the opposite, positively charged end of the gel. The gels were run at constant current of 16mA per gel for 7cm gels and 10mA for 17cm gels, at 200 Volts. When the dye front created by the Bromophenol Blue present in the agarose overlay had reached the bottom portion of the gels, electrophoresis was complete. The approximate run time for 7cm gels was 45 minutes, while the run time for 17cm gels was 18 hours (1cm/hr). The gels were carefully detached from the glass gel plates, specific corners of the gel were removed for identification and orientation purposes, and the gels are fixed in High destain.

Coomassie and SYPRO[®] staining:

Protein maps were detected by immersion of gels in Coomassie Brilliant Blue (5% Coomassie brilliant blue G-250, 45% methanol, 10% acetic acid) or a highly sensitive SYPRO[®] Ruby protein gel stain (1X pre-mixed solution) which allows for visualization of protein spots under an ultraviolet light. For Coomassie staining, the gels were directly transferred to plastic vessels containing a sufficient volume of Coomassie for full immersion of gels. The gels were stained overnight on an orbital shaker. The following day, the gels were subjected to High Destaining (40% methanol, 10% acetic acid) for 60 minutes and low de-staining (10% methanol, 6% acetic acid) until background was clear. Gels were then stored in ddH₂O for a minimum of 15 minutes before imaging.

For SYPRO[®] Ruby protein gel staining, the gels were directly transferred into plastic vessels containing SYPRO Fixing Solution/High Destain (40% methanol, 10% acetic acid) for 60 minutes. The fixing solution was discarded and the gels were fully immersed in a sufficient volume of SYPRO[®] stain. The gels were stained overnight on an orbital shaker. The following day, the gels were washed in deionized/distilled H₂O on the orbital shaker for a minimum of 15 minutes before imaging.

PDQuest[™] Imaging and Analysis:

The PDQuest[™] 2-D Analysis Software includes the Bio-Rad Gel Doc equipped with a CCD camera in which acquired images of the completed two-dimensional (2D) gel can be analyzed, optimized, and printed onto a video, digital, or local printer. To acquire digital images of gels subjected to 2DGE, gels were placed onto the Gel Doc, scanned,

and focused until visible edges had disappeared. A ruler was placed adjacent the gel to ensure clarity of gel. The white tray and Epi-White light were utilized for Coomassie-stained gels, while the UV box and Trans-UV light were utilized for SYPRO[®] stained gels. Both types of gels required Auto Exposure of the gel to find the best-fit image. When satisfied with image quality, the raw images were printed on a Sony printer and saved under specific file names.

Using the PDQuest[™] 2-D Analysis Software, specific portions of the gels containing the protein spots, excluding the dye fronts, were cropped. Crop settings were created, saved and applied to gels of the same condition to create a primary MatchSet. The gel with the best clarity was chosen as the Master image for that MatchSet. Automated detection and matching allowed for the detection and quantitation of spots of interest in all of the gels of the MatchSet. The Spot Detection Wizard allowed for both identification and quantitation of specific spots of interest, with such key tools as Edit Spot Tools and Match Tools. Multiple Higher Level MatchSets were created for further comparison of each time point, of both treated (1 μ M testosterone) and untreated differentiated C2C12 myoblasts.

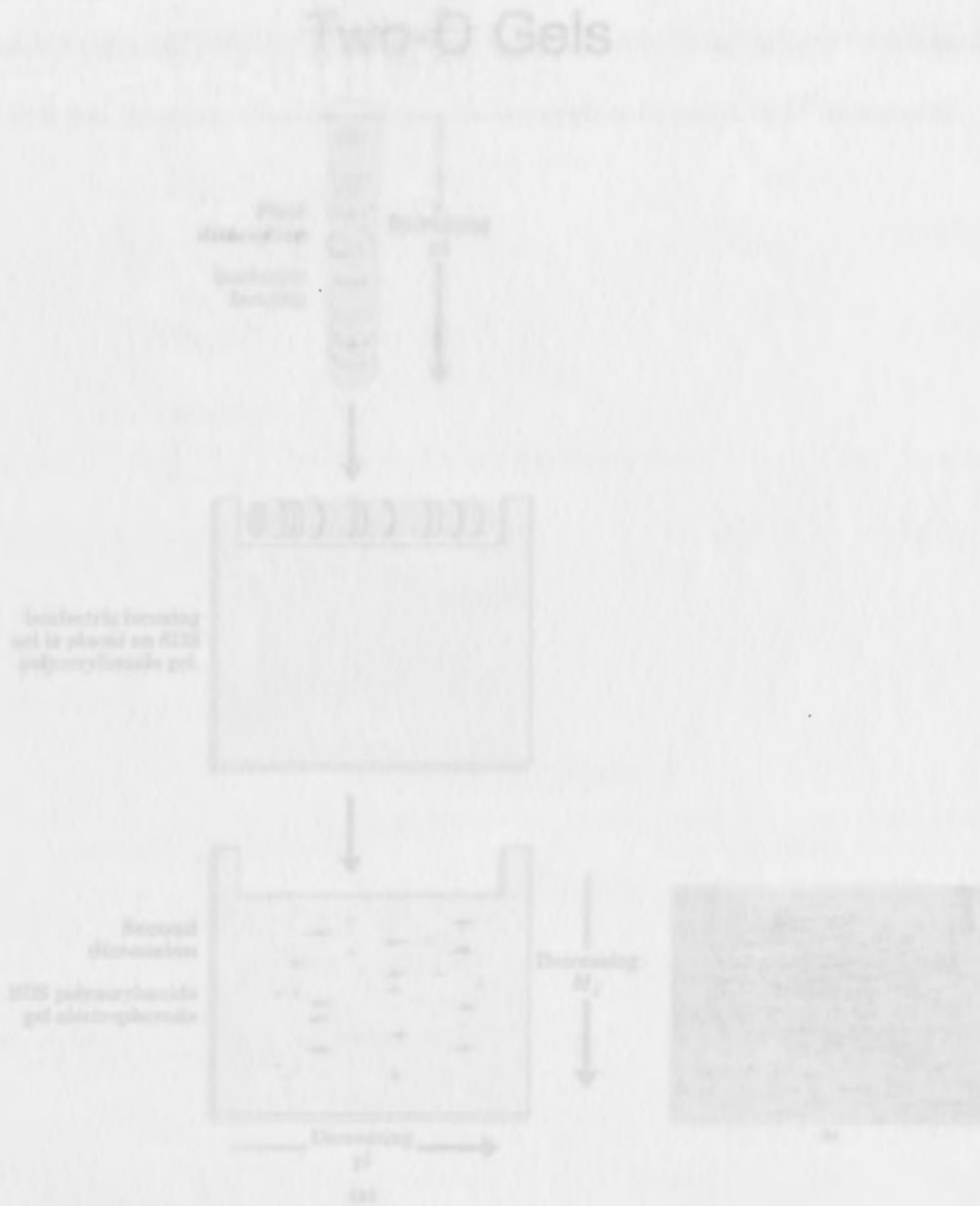
Mass Spectrometry and Bioinformatics:

Mass spectrometry (MS) is an important tool for the identification of specific proteins of interest. Determination of specific protein characteristics requires analysis of the peptides resulting from enzymatic lysis of the targeted protein (Beranova-Giorgianni 2003). Mass spectrometry delivers a “peptide mass fingerprint,” defining the mass of all peptides in the protein of interest. Secondly, the MS technique can fragment peptides

into product ions, and label the product ions with a “sequence tag” to aid in the exact identification of the protein of interest. Experimental data is then compared to the theoretical data and subjected to proteome analysis through database search programs such as SWISSPROT, PeptIdent, MultiIdent MS-Fit, MS-Tag, and MASCOT (Beranova-Giorgianni 2003).

Figure 2.1: Two-Dimensional Gel Electrophoresis

Depicts the process of 2DGE: Isoelectric focusing and 2D-PAGE

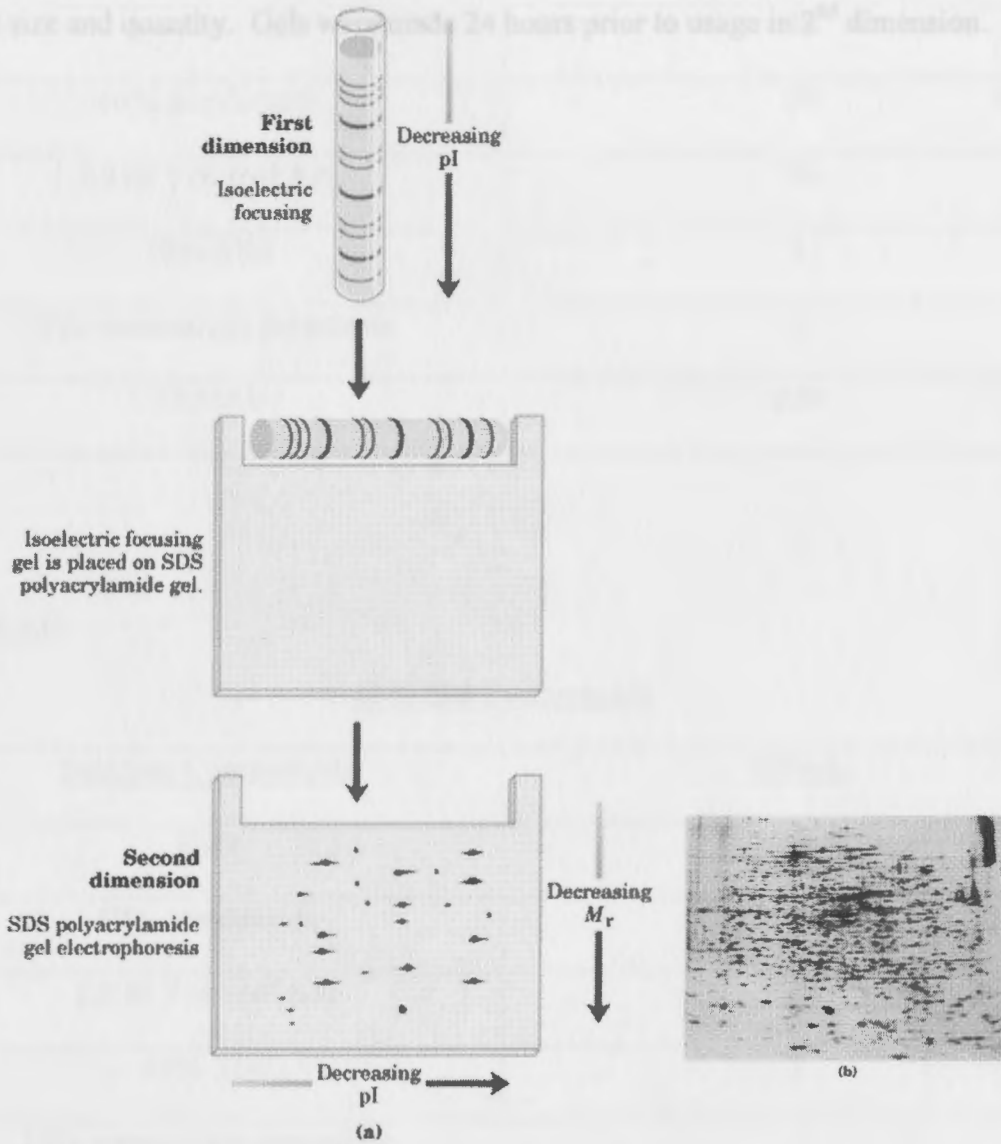


www.com.slu.se/~ahol/Robertson/overlappning.htm

Figure 2.1 Polyacrylamide Gel Components

Table 2.1a and Table 2.1b display compositions required for 10% and 12% polyacrylamide gel-making protocol yielding 100 and 120 mm x 100 mm gels. Total volume varied according to gel size and quantity. Gels were stored 24 hours prior to usage in 2nd dimension.

Two-D Gels



www.cm.utexas.edu/.../Robertus/overheads.htm

Table 2.1 Polyacrylamide Gel Components

Table 2.1a and Table 2.1b display components required for 10% and 12% polyacrylamide gel-making protocol yielding a 100 milliliter total volume. Total volume varied according to gel size and quantity. Gels were made 24 hours prior to usage in 2nd dimension.

40% acrylamide	25
1.5 M Tris (pH 8.8)	25
10% SDS	1
10% ammonium persulfate	1
TEMED	0.04

Table 2.1b

12% Gel Components

<u>Solution Components</u>	<u>100ml.</u>
H ₂ O	43
40% acrylamide	30
1.5 M Tris (pH 8.8)	25
10% SDS	1
10% ammonium persulfate	1
TEMED	0.04

Table 2.1a**10% Gel Components**

<u>Solution Components</u>	<u>100mL</u>
H₂O	48
40% acrylamide	25
1.5 M Tris (pH 8.8)	25
10% SDS	1
10% ammonium persulfate	1
TEMED	0.04

Table 2.1b**12% Gel Components**

<u>Solution Components</u>	<u>100mL</u>
H₂O	43
40% acrylamide	30
1.5 M Tris (pH 8.8)	25
10% SDS	1
10% ammonium persulfate	1
TEMED	0.04

Sample Preparation and 2D-Gel Results

All resulting data obtained from this study was achieved by previously described methods. As an overview, C2C12 cells were cultured appropriately and supplemented with differentiation media at 70-90% confluency. Triplicate samples of differentiated cells (untreated) were harvested at 0h, T=4h and T=24h time points and subjected to 2DGE. The experiment also included analysis of triplicate samples of C2C12 cultures supplemented with a differentiation medium containing testosterone (treated) at the T=0h, T=4h and T=24h time points. Each gel image represents sample harvested from one flask. Both untreated (controls) and testosterone-treated (experimental) samples were subjected to further PDQuest imaging and analysis to investigate the effects of testosterone on protein expression. The resulting protein spots may indicate proteins involved in the unknown signaling cascades underlying myogenic differentiation in combination with testosterone treatment.

CHAPTER III:

RESULTS

Protein assays were conducted using BSA concentration standards. Concentrations were determined by comparing samples to a standard curve of increasing concentrations of BSA (Table 3.1). Both sets of values were needed for the construction of a linear Standard BSA Curve using Microsoft Excel's X-Y scatter plot, represented in Figure 3-1. The resulting equation of the line yielded an R^2 value of 0.9927, sufficient for the determination of unknown protein sample concentrations. Unknown protein sample concentrations for T1=0h, T2=4h, and T3=24h controls determined by Standard BSA Curve values are indicated in Table 3.2. Table 3.2 also indicates calculated sample load volumes for 7cm IPG strips in microchips based on a total volume of 125 microliters for 7cm IPG strips and a total amount of 200 microliters

Sample Preparation and 2D-Gel Results:

All resulting data obtained from this study was achieved by previously described methods. As an overview, C2C12 cells were cultured appropriately and supplemented with differentiation media at 70-80% confluency. Triplicate samples of differentiated cells (untreated) were harvested at the T=0h, T=4h and T=24h time points and subjected to 2DGE. The experiment also included analysis of triplicate samples of C2C12 cultures supplemented with a differentiation medium containing testosterone (treated) at the Te=0h, Te=4h and Te=24h time points. Each gel image represents sample harvested from one flask. Both untreated (controls) and testosterone-treated (experimental) samples were subjected to further PDQuest imaging and analysis to investigate the effects of testosterone on protein expression. The resulting protein maps may indicate proteins involved in the unknown signaling cascades underlying myogenic differentiation in combination with testosterone treatment.

Protein assays were conducted using BSA concentration standards. Concentrations were determined by comparing samples to a standard curve of increasing concentrations of BSA (Table 3.1). Both sets of values were recorded for the construction of a linear Standard BSA Curve using Microsoft Excel's X-Y scatter plot, represented in Figure 3.1. The resulting equation of the line yielded an R^2 value of 0.9927, sufficient for the determination of unknown protein sample concentrations. Unknown protein sample concentrations for T1=0h, T2=4h, and T3=24h controls determined by Standard BSA Curve values are indicated in Table 3.2. Table 3.2 also indicates calculated sample load volumes for 7cm IPG strips in microliters based on a total volume of 125 microliters for 7cm IPG strips and a total volume of 300 microliters

for 17cm IPG strips preceding active rehydration. The above procedures were repeated for all prepared samples (controls and experimental) which were sonicated accordingly and suspended in Sample buffer before subsection to 2DGE.

In early experimentation with collected protein samples, samples were not being sonicated prior to active rehydration and 2DGE. Unsonicated samples resulted in unidentifiable protein maps with excessive smearing or the absence of protein, due to insufficient cell lysis (Data not shown). Following sonication, samples yielded a more complete representation of protein expression upon differentiation demonstrated by gel images. Possibly due to the nature of the C2C12 type and the method of cell lysis, gels displayed both horizontal and vertical streaking, later digitally removed by the PDQuest analysis software. Speckling was also removed by PDQuest analysis software.

Following adequate experimentation with 7cm gels, three modifications to the 2DGE protocol for this study are present in resulting gel images. Firstly, the pH range for IPG strips was changed from a broad range of 3-10 to a narrow range of 4-7 for better visualization of proteins. Secondly, the polyacrylamide gel percentage was increased from 10% to 12% to better resolve. Thirdly, the IPG strip length was changed from 7cm to 17cm for better visualization of proteins and facilitated manipulation during PDQuest analyses. The larger gels seemed to have less artifacts.

The 2D-Gel image depicted in Figure 3.2 was the first sample following sonication, which resulted in defined protein spot configurations. Figure 3.2 therefore indicated successful cell lysis. For the 1st dimension, the 2D gel was passively hydrated at 40,000 V-hours using 100µg of protein on a 7cm, pH 3-10 IPG strip. Electrophoresis was performed on a 10% polyacrylamide gel using Bio-Rad's Mini-PROTEAN[®] 3 with a

running power of 16mA. The gel was stained in Coomassie Brilliant Blue stain and visualized by Bio-Rad's ChemiDoc equipment. As in Figure 3.2, all resulting gel images were oriented from left to right by an increasing pH range, and from top to bottom by decreasing molecular weight.

Better resolution of proteins detected by the highly-sensitive SYPRO[®] stain can be seen in resulting protein maps present in Figure 3.3. Figure 3.3 represents typical, untreated (7cm Controls) 2D-Gel images following the induction of differentiation at T1=0h, T2=4h and T3=24h time points. The 2D images are "Raw" images of the gels at each time point, meaning the gels images have not been altered by the PDQuest software. The color of the Raw image, however, can be modified by using the "Transform" feature, which will change the displayed color of the image to red, green, blue, gray etc. For the 1st dimension, the 2D gels were actively hydrated and run at 40,000 V-hours using 100µg of protein on 7cm, pH 4-7 IPG strips. Electrophoresis was performed on 12% polyacrylamide gels using Bio-Rad's Mini-PROTEAN[®] 3 with a running power of 16mA per gel and stained in SYPRO[®] Ruby protein gel stain. Protein spot configurations in the upper left and lower middle quadrants of the three gels demonstrate varying degrees of intensities and presence of proteins. Due to difficulty in generating MatchSets from 7cm gels using PDQuest software, manual comparison of spots was required for analysis.

Figure 3.4 represents typical, testosterone-treated (7cm Experimental) 2D-Gel images following induction of differentiation at 0h, 4h and 24h time points. Again, visual changes in the intensities of protein spot configurations in the lower middle quadrants of the three gels resulted. Methods for the 1st and 2nd dimensions were repeated, as described previously for Figure 3.3.

Table In order to achieve greater separation of protein, 2DGE was carried out using 17 cm IPG strips. The resulting 2D-Gel images represented in Figure 3.5 are typical, untreated (17cm Controls) following induction of differentiation at T=0h, T=4h and T=24h time points. The 2D images are “Raw” images actively hydrated at 60,000 V-hours using 400µg of protein on 17cm, pH 4-7 IPG strips. Electrophoresis was performed on 12% gels using Bio-Rad’s PROTEAN II XL Electrophoresis chamber with a running power of 10mA per gel and stained in SYPRO® Ruby protein gel stain. Gel images were later subjected to PDQuest analyses. Figure 3.6 represents typical, treated (17cm Experimental) following induction of differentiation at Te=0h, Te=4h, and Te=24h time points. Methods for the 1st and 2nd dimensions were repeated, as described previously for Figure 3.5.

Table 3.1: Modified Bradford Assay Concentrations and Absorbances

Concentrations of BSA in micrograms and resulting absorbances achieved at 595 nanometers of UV-Visible light, necessary for the construction of a linear Standard

BSA Curve to determine unknown sample concentrations.

Concentration (micrograms)	Absorbance (at 595 nanometers)
10	0.14259
15	0.20689
20	0.26526
25	0.28287
30	0.34491
35	0.39371
40	0.40752

Figure 3.1: Standard BSA Curve

Table 3.1

Figure 3.1 Modified Bradford Assay Concentrations and Absorbances

Standard BSA Concentration (micrograms)	Absorbance (at 595 nanometers)
10	0.14259
15	0.20089
20	0.26526
25	0.28287
30	0.34491
35	0.39321
40	0.40752

Figure 3.1

Figure 3.1: Standard BSA Curve

Figure 3.1 represents a linear Standard BSA Curve based upon the absorbance of standard BSA concentrations (10.3 μg) at 10, 15, 20, 25, 30, 35, and 40 increments versus the absorbance of the protein dye complex at 595nm. The Standard BSA Curve allowed for quantitation of an appropriate protein sample load for ReadyStrip™ IPG strips.



Figure 3.1 Sample Protein Concentration

The table represents unknown protein protein concentrations in micrograms/microliters

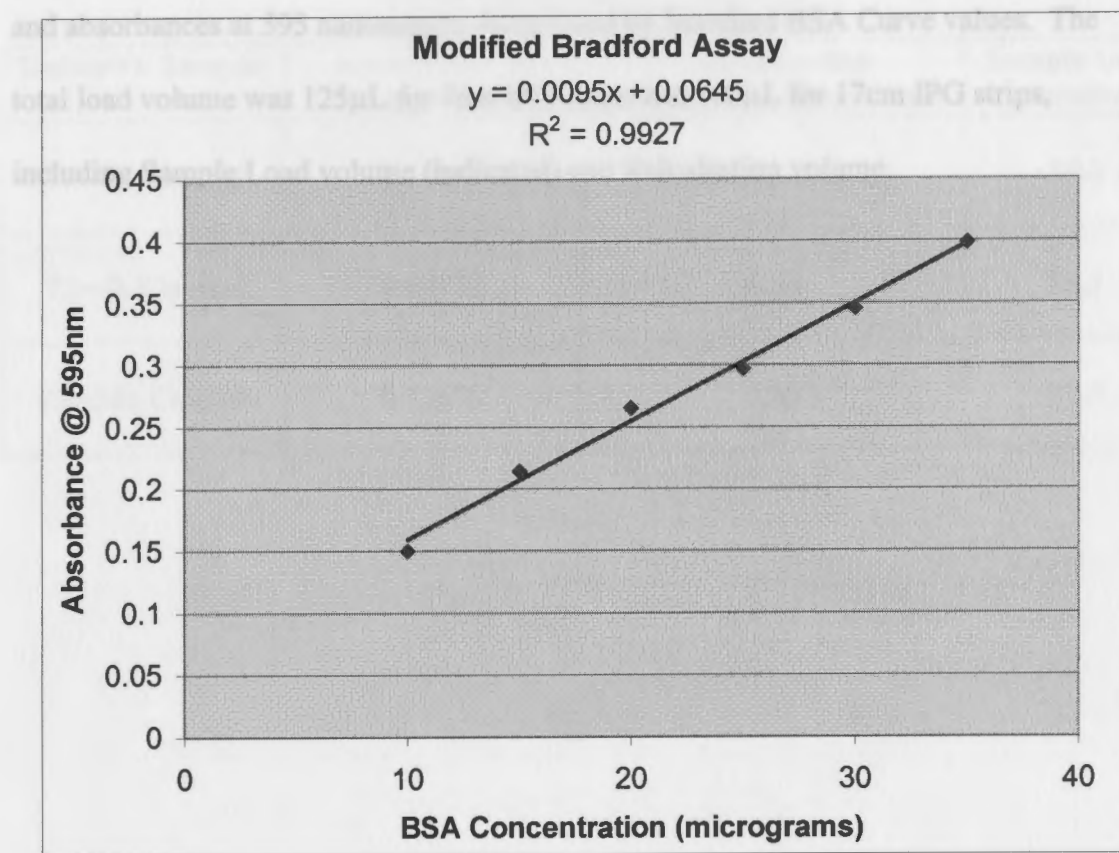


Table 3.2: Sample Protein Concentrations

The table represents unknown sample protein concentrations in micrograms/microliters and absorbances at 595 nanometers determined by Standard BSA Curve values. The

Unknown Sample	Absorbance at 595 nm	Concentration (µg/µL)	Sample Load (µL)
			17.3
T2~4h Control	0.60738	6.54	15.3
T3~24h Control	0.52579	5.60	17.9

Table 3.2 2D-Gel Images (Test Control)

Represents untreated two-dimensional gel image (Raw) at the 0h time point. For this 1st dimension the 2D-gel was initially hydrated at 40/80 V-hours using 100µg of protein

Sample Protein Concentrations

Unknown Sample	Absorbance at 595 nanometers	Concentration (micrograms/microliters)	Sample Load (microliters)
T1=0h Control	0.54095	5.78	17.3
T2=4h Control	0.60758	6.54	15.3
T3=24h Control	0.52579	5.60	17.9

Figure 3.2: 2D-Gel Image (7cm Control)

Represents untreated two-dimensional gel image (Raw) at the 0hr time point. For the 1st dimension, the 2D-gel was actively hydrated at 40,000 V-hours using 100µg of protein on 7cm, pH 3-10 IPG strip. Electrophoresis was performed on a 10% polyacrylamide gel using Bio-Rad's Mini-PROTEAN[®] 3 with a running power of 16mA and stained in Coomassie Brilliant Blue stain. The gel image was not subjected to PDQuest analysis.

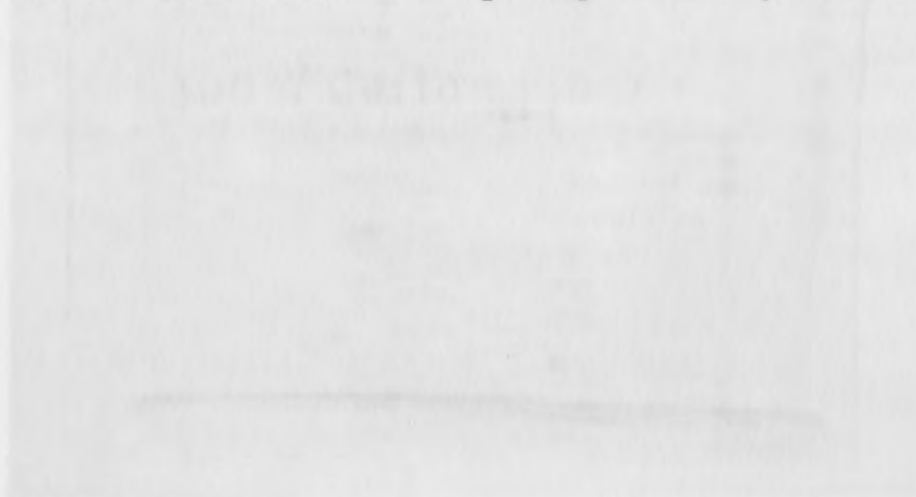


Figure 3.2: 2D-Gel Images (7cm Control)

Represents typical, uninduced two-dimensional gel images (Raw) following induction of differentiation at T=0h (7cm control) (top), and T3=24h (bottom) time points.

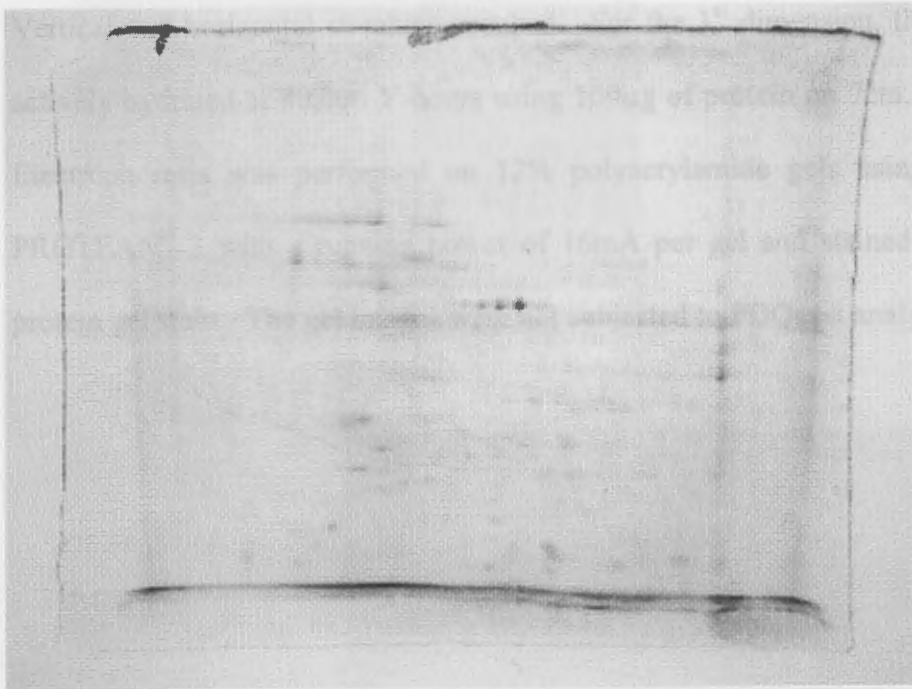


Figure 3.3: 2D-Gel Images (7cm Controls)

Represents typical, untreated two-dimensional gel images (Raw) following induction of differentiation at T1=0h (top), T2=4h (middle), and T3=24h (bottom) time points. Vertical and horizontal streaking resulted. For the 1st dimension, the 2DGE gels were actively hydrated at 40,000 V-hours using 100µg of protein on 7cm, pH 4-7 IPG strips. Electrophoresis was performed on 12% polyacrylamide gels using Bio-Rad's Mini-PROTEAN[®] 3 with a running power of 16mA per gel and stained in SYPRO[®] Ruby protein gel stain. The gel images were not subjected to PDQuest analyses.

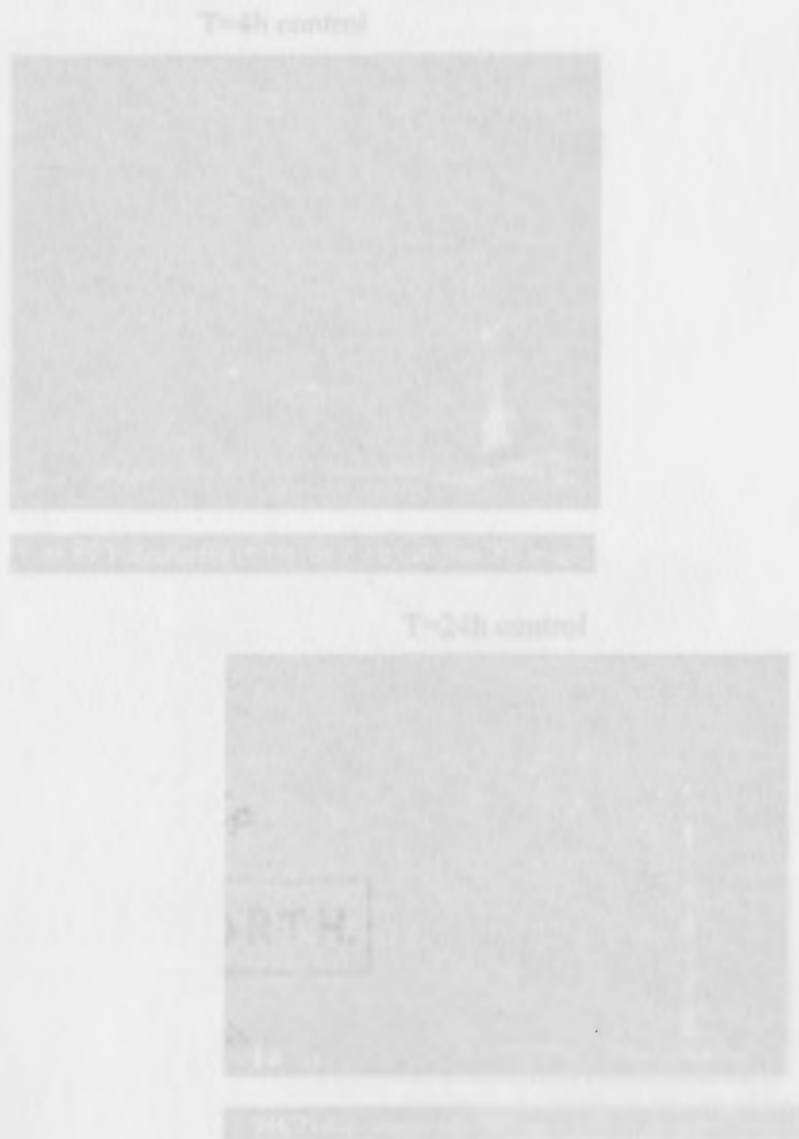


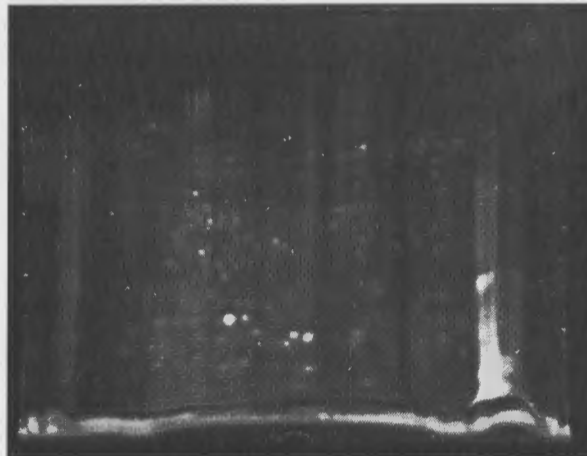
Figure 3.3

T=0h control



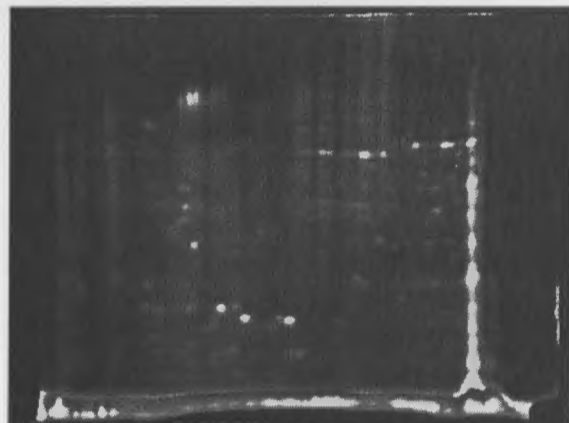
T=0 17.3 ul collected (1-14) run 2-2-05 v1 (Raw 2-D Image)

T=4h control



T=4h 15.3 ul collected (1-14) run 2-2-05 v1 (Raw 2-D Image)

T=24h control



T=24h 35.8ul collected (1-15) run 3-3-05 v1 (Raw 2-D Image)

Figure 3.4 2D-Gel Images (7cm Experimental)

Represents typical, treated (experimental) two-dimensional gel images following induction of differentiation at Te1=0h (top), Te2=4h (middle), and Te3=24h (bottom) time points. Vertical streaking resulted. For the 1st dimension, the 2DGE gels were actively hydrated at 40,000 V-hours using 100µg of protein on 7cm, pH 4-7 IPG strips. Electrophoresis was performed on 12% polyacrylamide gels using Bio-Rad's Mini-PROTEAN[®] 3 with a running power of 16mA per gel and stained in SYPRO[®] Ruby protein gel stain. The gel images were not subjected to PDQuest analyses.

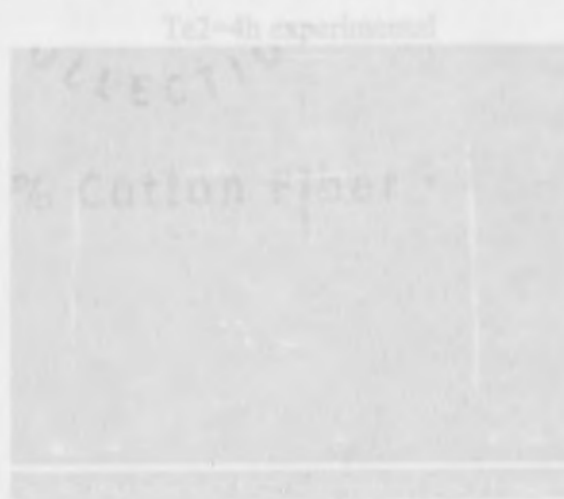
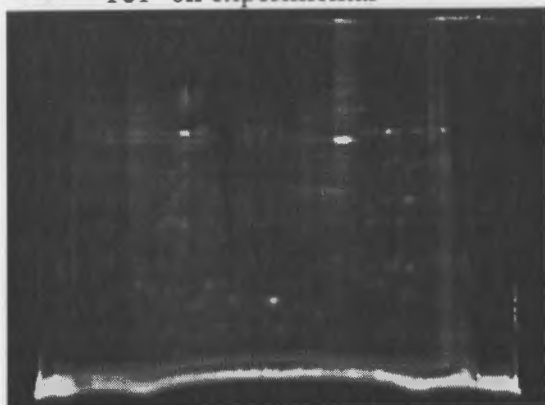


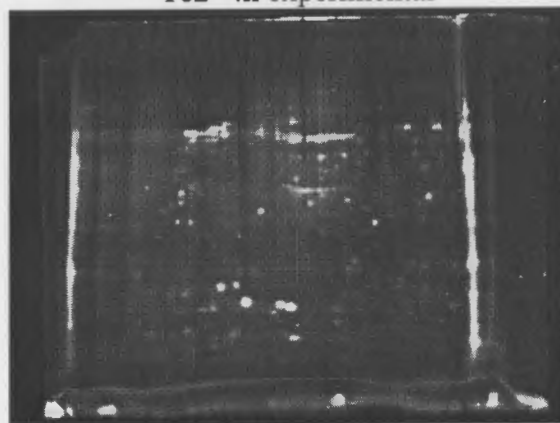
Figure 3.4 2D-Gel Images (17um Control)

Te1=0h experimental



Te1=0h 29.3ul collected 1-14-05 run 3-3-05 v1 (Raw 2-D Image)

Te2=4h experimental



Te2=4h 26 ul collected 1-14-05 run 2-15-05 v1 (Raw 2-D Image)

Te3=24h experimental



Te3=24h 15.1ul collected 1-15-05 run 2-15-05 v1 (Raw 2-D Image)

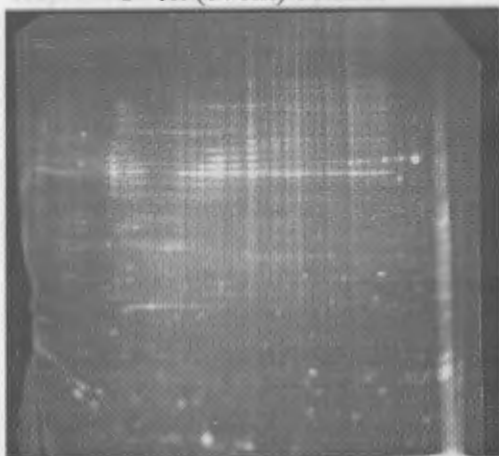
Figure 3.5 2D-Gel Images (17cm Controls)

Represents untreated (Controls) two-dimensional gel images following induction of differentiation at T1=0h (top), T2=4h (middle), and T3=24h (bottom) time points. Vertical and horizontal streaking resulted. For the 1st dimension, the 2DGE gels were actively hydrated at 60,000 V-hours using 400 μ g of protein on 17cm, pH 4-7 IPG strips. Electrophoresis was performed on 12% polyacrylamide gels using PROTEAN II XL Electrophoresis chamber with a running power of 10mA per gel and stained in SYPRO[®] Ruby protein gel stain. The gel images were later subjected PDQuest analyses.



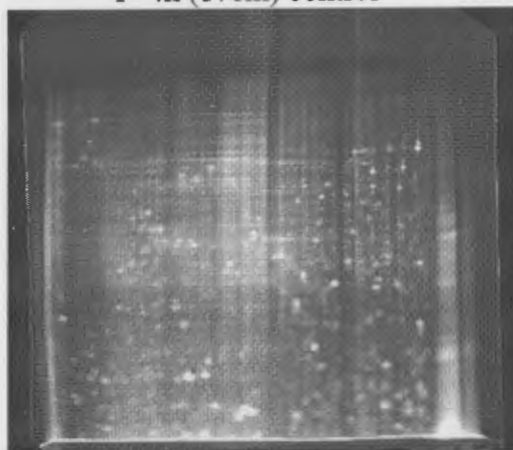
Figure 3.5 2D-Gel Images (17cm) (Continued)

Representative 2D-gel images following induction of ... (middle), and T=24h (bottom) time points.



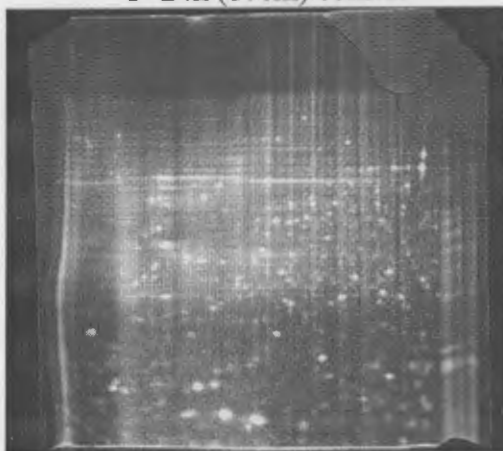
T=0 (17cm) 70ul collect 1-14 run 4-20-05 v1 (Raw 2-D Image)

T=4h (17cm) control



T=4h (17cm) collect 1-14 run 4-21-05 v1 (Raw 2-D Image)

T=24h (17cm) control



T=24h (17cm) collect 1-15 run 4-21-05 v1 (Raw 2-D Image)

Figure 3.6 2D-Gel Images (17cm Experimental)

Represents treated (Experimental) two-dimensional gel images following induction of differentiation at $T_{e1}=0h$ (top), $T_{e2}=4h$ (middle), and $T_{e3}=24h$ (bottom) time points. Vertical streaking resulted. For the 1st dimension, the 2DGE gels were actively hydrated at 60,000 V-hours using 400 μ g of protein on 17cm, pH 4-7 IPG strips. Electrophoresis was performed on 12% polyacrylamide gels using PROTEAN II XL Electrophoresis chamber with a running power of 10mA per gel and stained in SYPRO[®] Ruby protein gel stain. The gel images were later subjected PDQuest analyses.



Figure 3.6

Te7=0h (17cm) experimental



Te7-0h (17cm) collect 1-14 run 4-20-05 v1 (Raw 2-D Image)

Te8=4h (17cm) experimental



Te8-4h (17cm) 70ul collect 1-14 run 3-25-05 v1 (Raw 2-D Image)

Te6=24h (17cm) experimental



Te6-24h (17cm) 76ul run 4-21-05 v1 (Raw 2-D Image)

PDQuest Analyses:

Gel images obtained from 17cm two-dimensional gels were subjected to further PDQuest analyses to ultimately examine changes in qualitative and quantitative protein expression possibly linked to differentiation in combination with testosterone administration. Images obtained from testosterone-treated (experimental) and untreated (control) triplicate samples were cropped accordingly to create "MatchSets." Primary "MatchSets" from each time point were created and protein spot configurations were observed in 3x3 quadrants of the gel. Gel images were also manually edited to remove false recordings of spots caused by frequent tearing of gels, vertical and horizontal streaking, and speckling. Matching summaries indicate the number of matched and unmatched spots, and are reflected in match percentages. "Match Rate 1" indicates match percentages relative to total spots on the gel, while Match Rate 2 indicates match percentages relative to the total spots on the Master. Synthetic "Master" images containing all spot data from gels in the primary MatchSet were then used to create "Higher Level MatchSets." Higher Level MatchSets (HLM) created from primary MatchSets were necessary for Master image comparison of matched and unmatched spots.

Figures 3.7-3.11 demonstrate resulting MatchSet summary data obtained from 0h, 4h and 24h time points of testosterone-treated (experimental) and untreated (controls) gel images, with the Master images displayed in the upper left region. Because the gels of each MatchSet were derived from the same conditions, gel match percentages should be nearly 100%. Resulting MatchSet data yielded lower, less consistent match percentages. The T4h (Figure 3.8) and T24h (Figure 3.9) control MatchSets demonstrated the lowest

matching percentages, while the Te4h (Figure 3.10) experimental MatchSets yielded the highest match percentages. When MatchSets were created from gel images with the lowest match percentages, T4h and T24h, the PDQuest software required a digital inversion of the Master gel image spots due to spot quantities. HLM created from those MatchSets yielded 0% match rates, inconsistent with visual assessment of gel images.

Figure 3.12 represents resulting HLM summary data from the T0h Control MatchSet (Figure 3.7) and the Te4h Experimental MatchSet (Figure 3.10) with T0h chosen as the Master image for comparison. Matched spots were identified by green letters, while unmatched spots were identified by red ellipses in Figure 3.13. HLM summary data yielded 85 unmatched spots and 68 matched spots between the two gel images, suggesting 85 differential proteins between the T0h control and the Te4h testosterone-treated samples. Figure 3.14 demonstrates the 85 unique proteins to the Te4h time point indicated by red ellipses.

Because of inconsistent HLM data resulting from a T4h and Te4h comparison, a manual comparison of Te4h and T4h MatchSet data was performed (Figure 3.15). When the crop settings for the T4h Control MatchSet were created, a crosshair was placed on a spot present in all three gel images. Those exact crop settings, were then loaded onto the three gel images to create the Te4h Experimental MatchSet. The spot was then identified as the same spot present in the two conditions, due to the crosshair located directly on that spot. A three-spot and two-spot configuration was then compared using the MatchTool feature "Show Match", indicated by yellow squares. Figure 3.15 demonstrates a three-spot configuration in the 3x3 lower right quadrant of the T4h Control MatchSet containing a unique spot (highlighted by yellow squares). Also

demonstrated in Figure 3.15 is the corresponding two-spot configuration in the 3x3 lower right quadrant of the Te4h Experimental MatchSet lacking the unique spot, in which the area lacking the spot is indicated by a red arrow in the Master image and raw image.

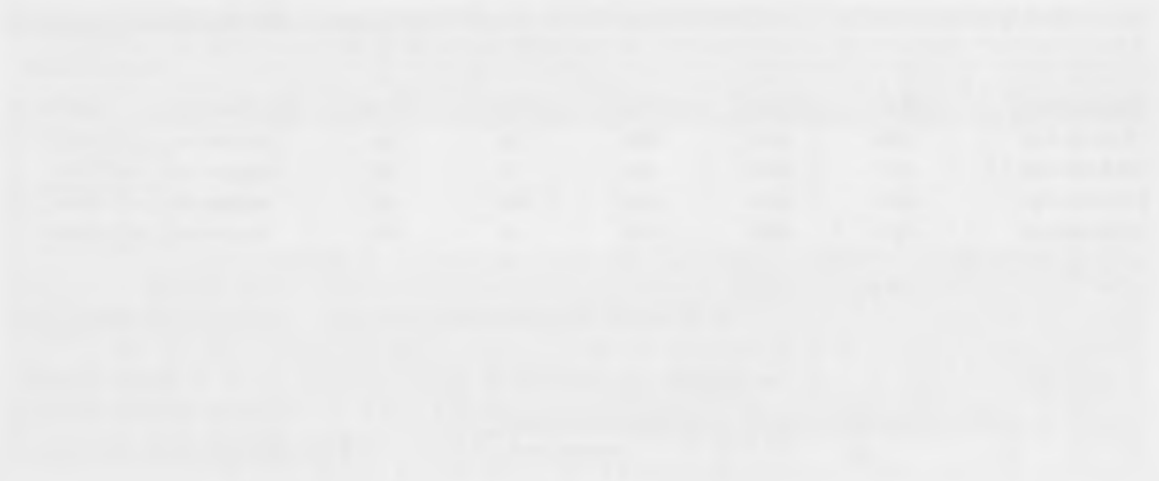
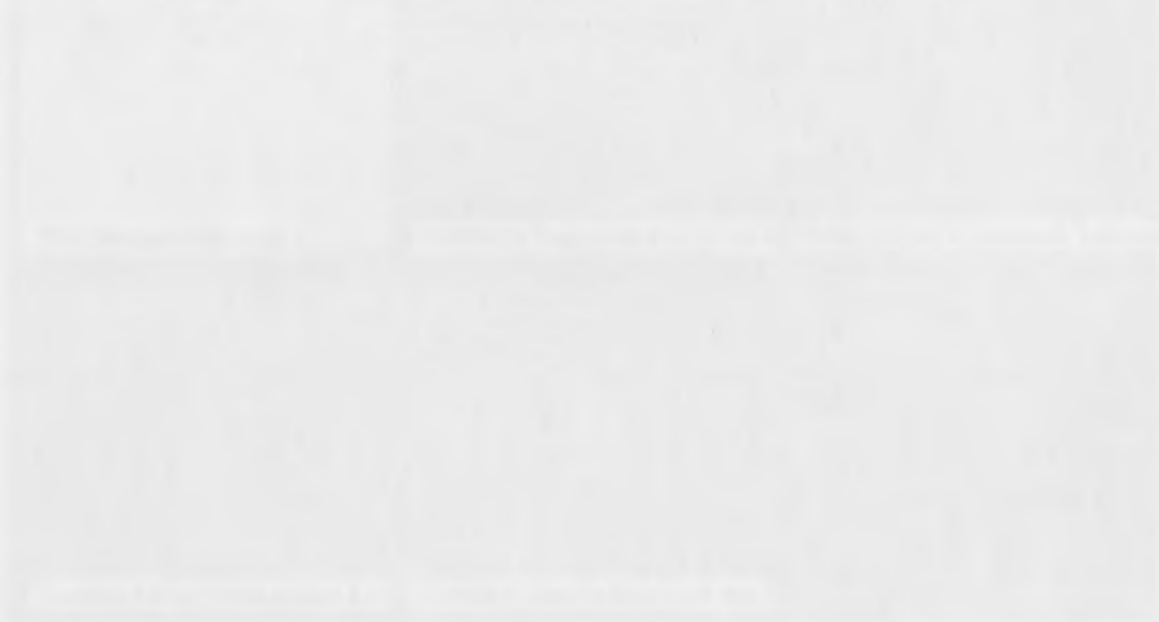


Figure 3.7 PDQuest Analysis-T0h Control MatchSet

Represents MatchSet summary data obtained from four, zero-hour time points: T=0h, Te1=0h, Te4=0h and Te7=0h. Te1=0h was chosen as the Master image.



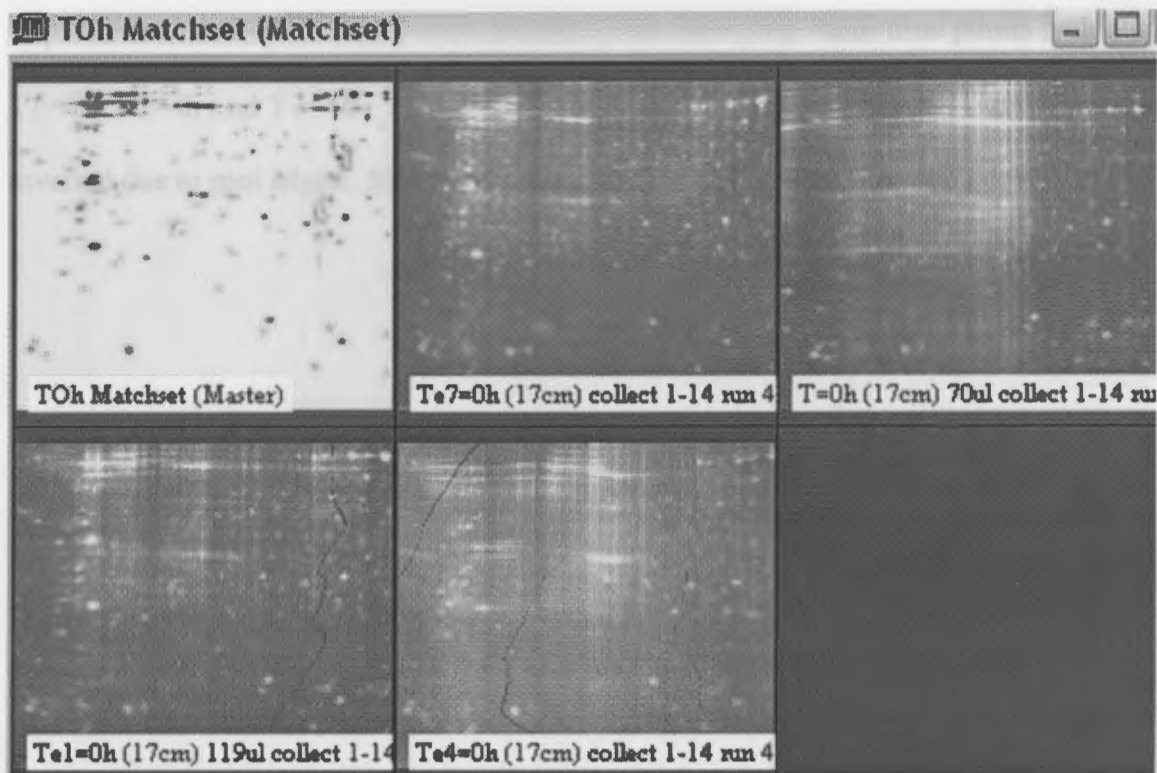
MatchSet Summary for T0h Control

File Name	Product Image	T Time	Matched	Match Time %	Match Size %	Core Count	Core Location
T=0h (17mm)	not assigned	100	36	32%	37%	0.001	T=0h Control 1
T=0h (17mm)	not assigned	100	12	20%	30%	0.001	T=0h Control 2
T=0h (17mm)	not assigned	100	118	100%	100%	1.000	T=0h Control 3
T=0h (17mm)	not assigned	200	26	27%	20%	0.002	T=0h Control 4

Matched with * Confirmed coefficient based on T=0h Control 1

Matched	Matched	Matched	Matched
36	12	118	26
32%	20%	100%	27%
37%	30%	100%	20%
0.001	0.001	1.000	0.002

Figure 3.7



Matching Summary for 'TOh Matchset'

Member information

Gel Name	Replicate Group	Spots	Matched	Match Rate 1	Match Rate 2	Corr Coeff	Detect paramet
Te7=0h (17cm...	not assigned	165	96	58%	50%	0.801	TOh PARAMETE
T=0h (17cm) ...	not assigned	189	72	38%	38%	0.511	TOh PARAMETE
Te1=0h (17cm...	not assigned	189	189	100%	100%	1.000	TOh PARAMETE
Te4=0h (17cm...	not assigned	203	56	27%	29%	0.269	TOh PARAMETE

Master is marked with * Correlation coefficient based on Te1=0h (17cm) 1..

MatchSet information

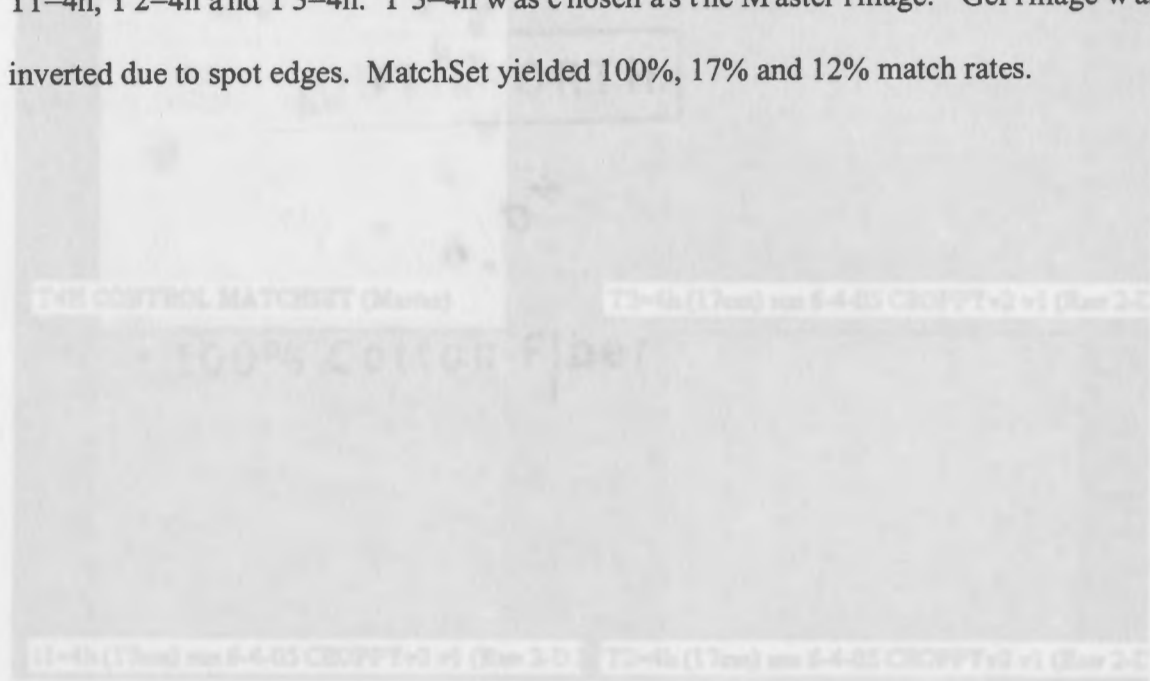
Spots matched to every member:	29
Overall mean coefficient of variation:	43.28

Replicate group and classes information

Replicate Group/Classes	Member	Matched to all	Mean CV
all not assigned	4	29	43.26

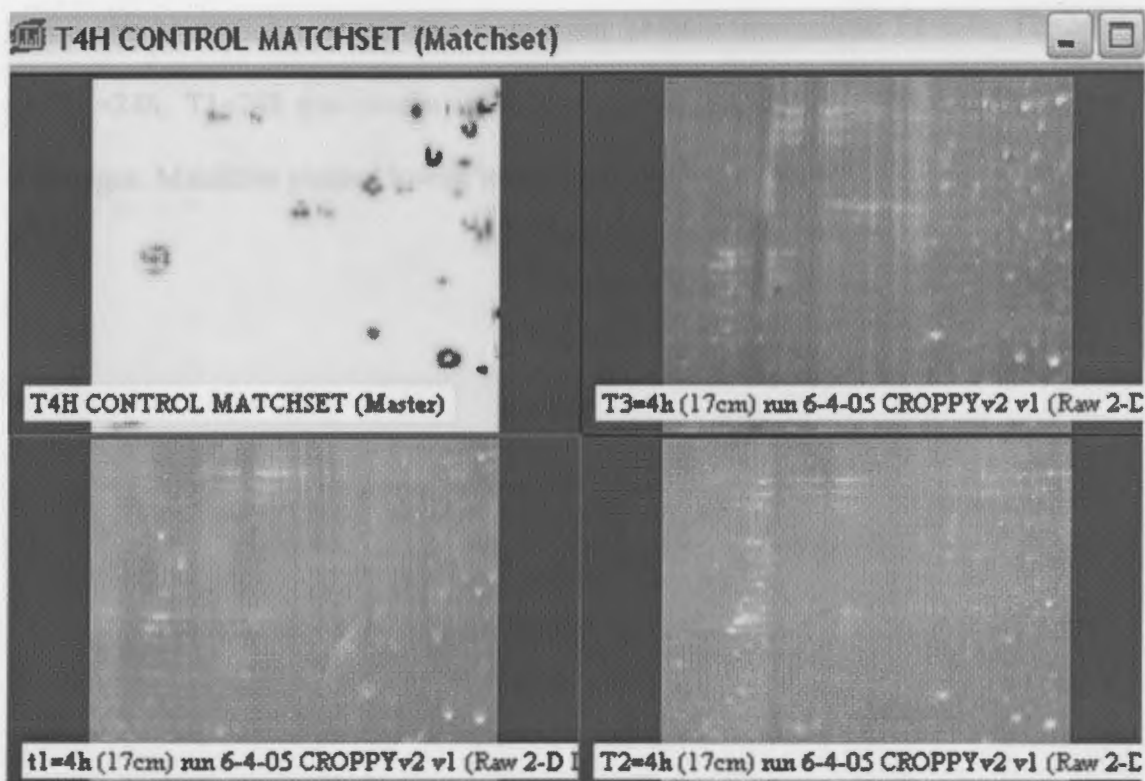
Figure 3.8 PDQuest Analysis-T4h Control MatchSet

Represents MatchSet summary data obtained from three, four-hour time points including T1=4h, T2=4h and T3=4h. T3=4h was chosen as the Master image. Gel image was inverted due to spot edges. MatchSet yielded 100%, 17% and 12% match rates.



MatchSet	Matched Spots	Total Spots	Match Rate	Matched Spots	Total Spots	Match Rate	Matched Spots	Total Spots	Match Rate
T1=4h (17min) run 6-4-05 CROFFT+3 v1 (Row 2-D)	32	32	100%	1279	1280	99.9%	328	328	100%
T2=4h (17min) run 6-4-05 CROFFT+2 v1 (Row 2-C)	7	41	17%	130	1080	12%	328	328	100%
T3=4h (17min) run 6-4-05 CROFFT+2 v1 (Row 2-C)	37	37	100%	286	2340	12%	328	328	100%

Figure 3.8



Matching Summary for "T4H CONTROL MATCHSET"

Member information

Gel Name	Replicate Group	Spots	Matched	Match Rate 1	Match Rate 2	Corr Coeff	Detect paramet
T3=4h (17cm)...	not assigned	62	62	100%	100%	1.000	T4H CONTROL
t1=4h (17cm)...	not assigned	71	9	12%	14%	0.665	T4H CONTROL
T2=4h (17cm)...	not assigned	87	15	17%	24%	0.149	T4H CONTROL

Master is marked with * Correlation coefficient based on T3=4h (17cm) ru..

MatchSet information

Spots matched to every member:	9
Overall mean coefficient of variation:	31.89

Replicate group and classes information

Replicate Group/Classes	Member	Matched to all	Mean CV
all not assigned	3	9	31.89

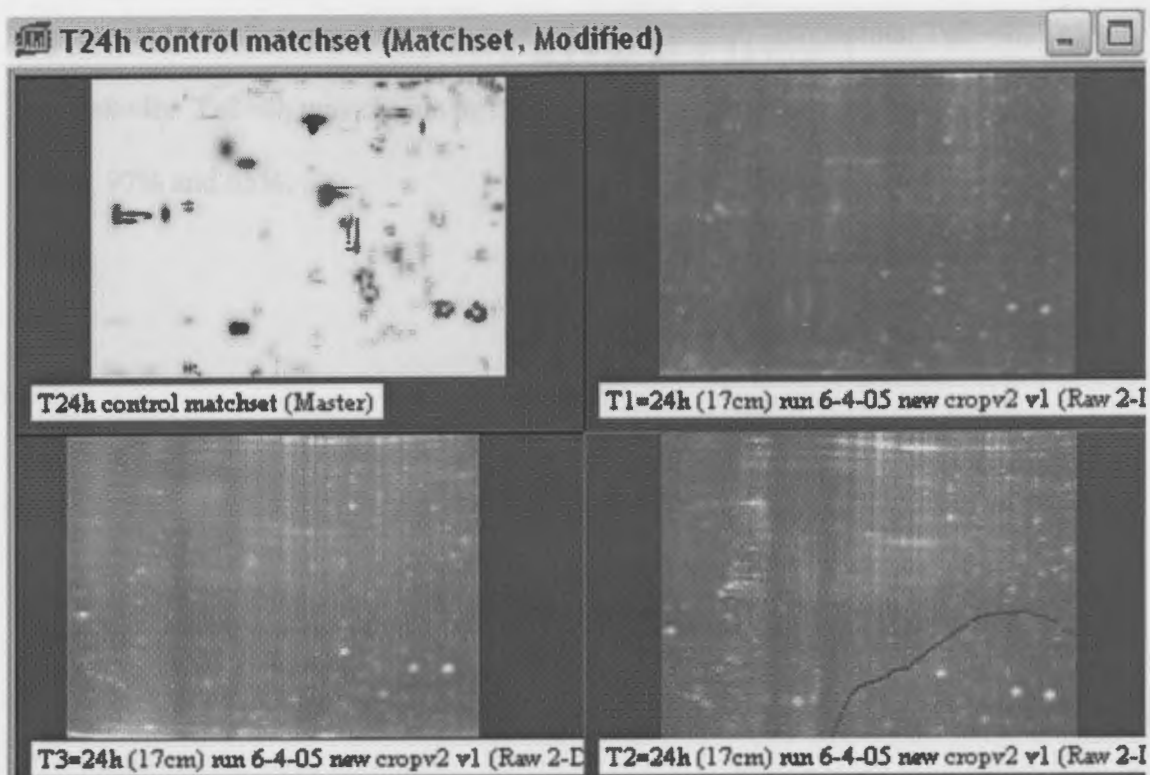
Figure 3.9 PDQuest Analysis-T24h Control MatchSet

Represents MatchSet summary data from three, 24-hour time points: T1=24h, T2=24h and T3=24h. T1=24h was chosen as the Master image. Gel image was inverted due to spot edges. MatchSet yielded lowest match rates: 100%, 15% and 13%.



Run Name	Reference Image	Spots	Matched	Match Rate %	Change Rate %	Total Spots	Matched Spots
T1=24h (17ms)	not assigned	202	202	100%	100%	2,000	202
T2=24h (17ms)	not assigned	204	30	15%	85%	2,000	30
T3=24h (17ms)	not assigned	202	26	13%	87%	2,000	26

Figure 3.9



Matching Summary for "T24h control matchset"

Member information

Gel Name	Replicate Group	Spots	Matched	Match Rate 1	Match Rate 2	Corr Coeff	Detect paramet
*T1=24h (17cm...	not assigned	263	263	100%	100%	1.000	T24h parameter
T3=24h (17cm...	not assigned	374	52	13%	19%	0.294	T24h parameter
T2=24h (17cm...	not assigned	263	42	15%	15%	0.163	T24h parameter

Master is marked with * Correlation coefficient based on T1=24h (17cm) r..

MatchSet information

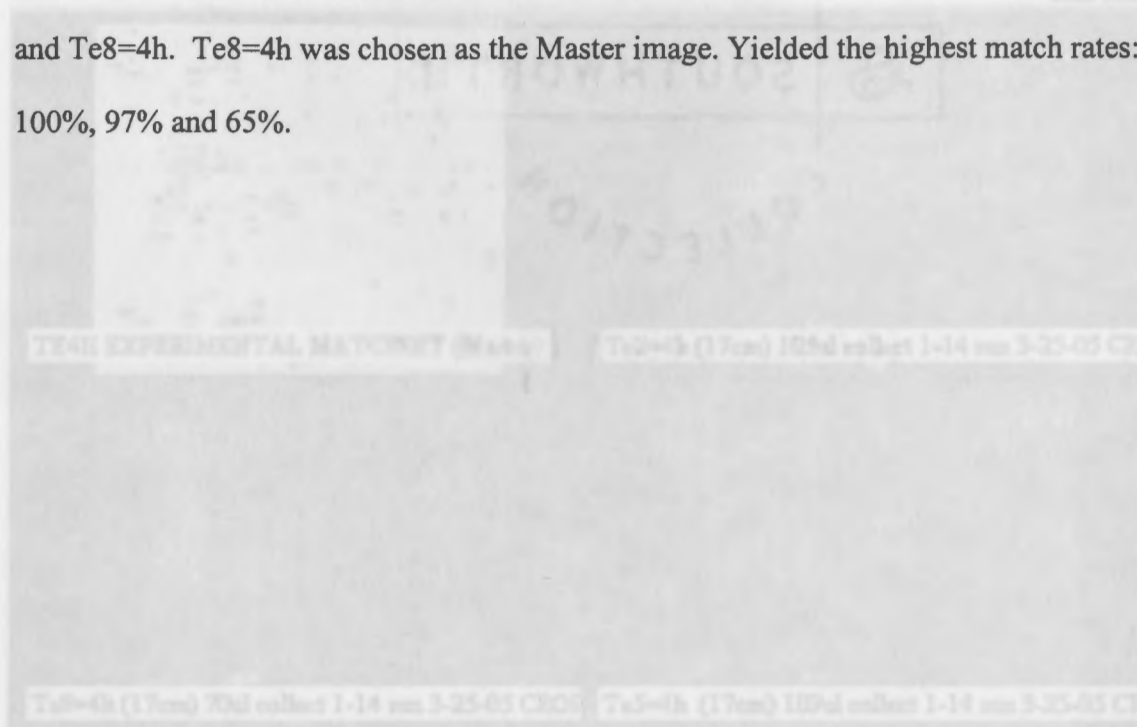
Spots matched to every member:	10
Overall mean coefficient of variation:	63.16

Replicate group and classes information

Replicate Group/Classes	Member	Matched to all	Mean CV
all not assigned	3	10	63.16

Figure 3.10 PDQuest Analysis-Te4h Experimental (Testosterone-treated) MatchSet

Represents MatchSet summary data from three, four-hour time points: Te2=4h, Te5=4h and Te8=4h. Te8=4h was chosen as the Master image. Yielded the highest match rates: 100%, 97% and 65%.



Summary Statistics for TE8=4h EXPERIMENTAL MATCHSET

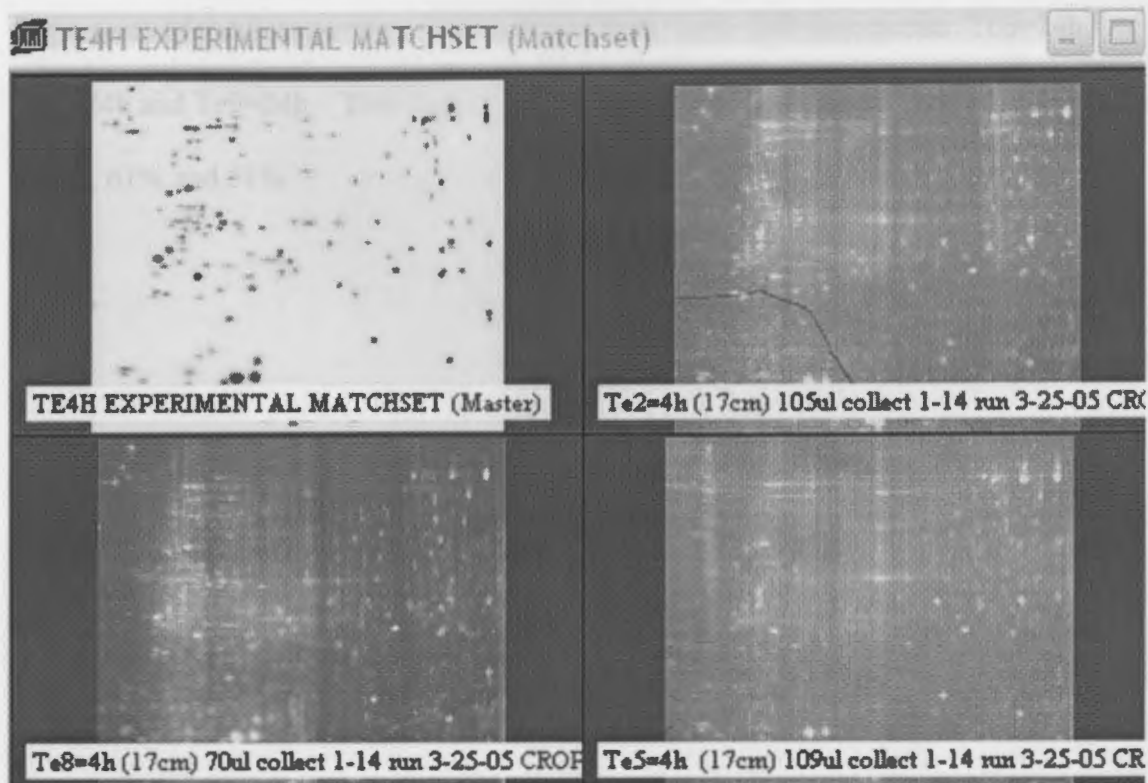
Match Rate	Matched	Total	Matched (%)	Total (%)	Matched (Count)	Total (Count)
100%	80	80	100%	100%	1000	1000

Matched: 80 / Total: 80

Matched: 80 / Total: 80

Matched: 80 / Total: 80

Figure 3.10



Matching Summary for "TE4H EXPERIMENTAL MATCHSET":

Member information

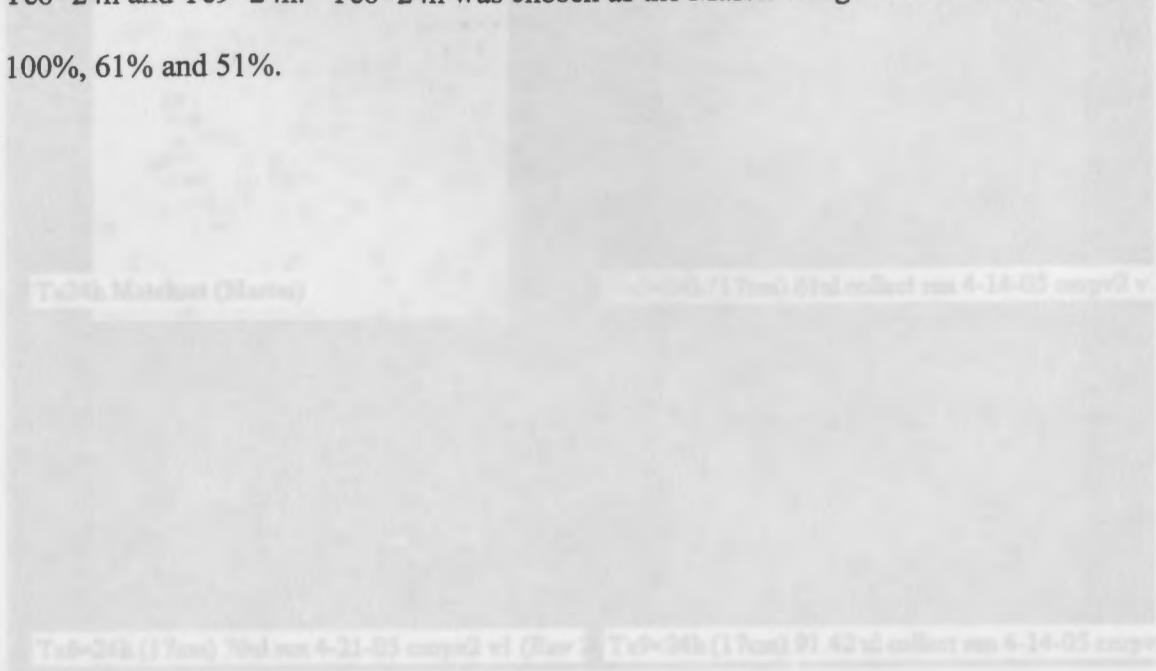
Gal Name	Replicate Group	Spots	Matched	Match Rate 1	Match Rate 2	Corr Coeff	Detect param
Te2=4h (17cm...	not assigned	140	92	65%	58%	0.878	Te4h EXPERIME
*Te8=4h (17cm...	not assigned	123	123	100%	77%	1.000	Te4h EXPERIME
Te5=4h (17c...	not assigned	94	92	97%	58%	0.653	Te4h EXPERIME

Master is marked with * Correlation coefficient based on Te8=4h (17cm) 7..

MatchSet information		Replicate group and classes information			
Spots matched to every member:	54	Replicate Group/Classes	Member	Matched to all	Mean CV
Overall mean coefficient of variation:	30.80	all not assigned	3	54	30.60

Figure 3.11 PDQuest Analysis-Te24h Experimental (Testosterone-treated) MatchSet

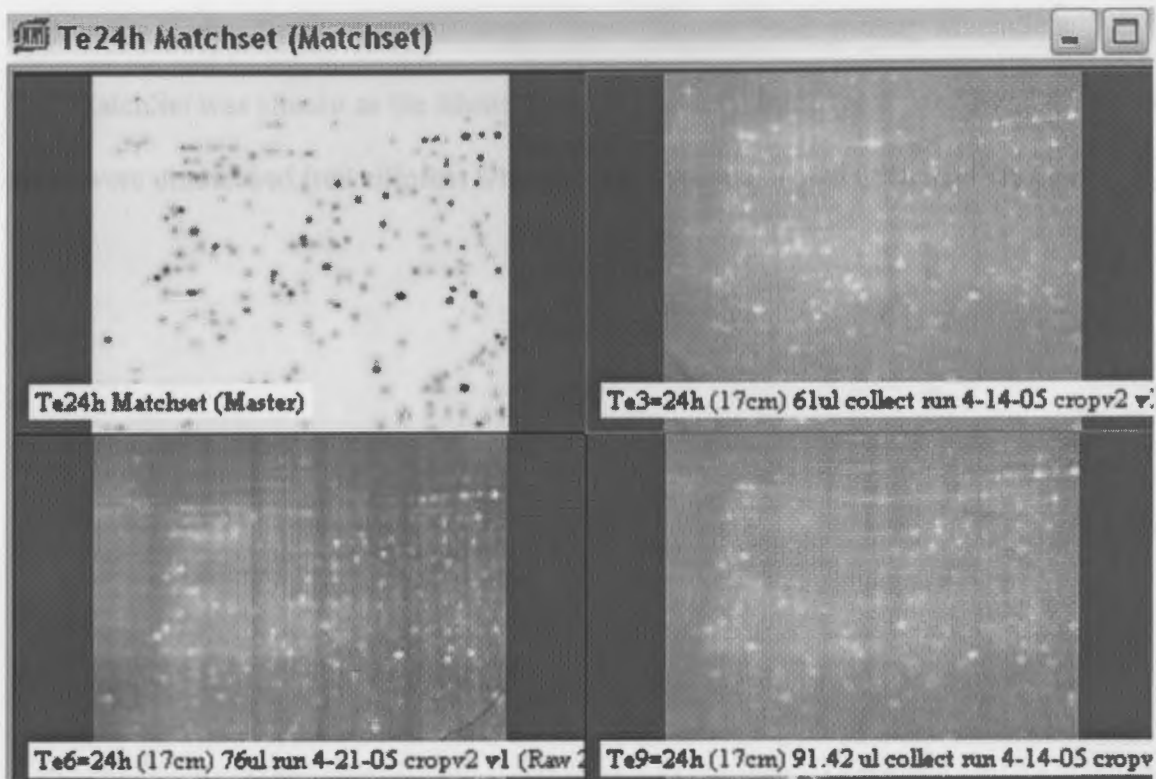
Represents MatchSet summary data obtained from three, 24h time points: Te3=24h, Te6=24h and Te9=24h. Te6=24h was chosen as the Master image. Yielded match rates: 100%, 61% and 51%.



Time Point	Match Rate	Total	Matched	Match Rate 1	Match Rate 2	Total	Matched
Te3=24h	100%	100	100	100%	100%	100	100
Te6=24h	61%	164	100	61%	100%	164	100
Te9=24h	51%	137	70	51%	100%	137	70

Match Set	Match Rate	Total	Matched	Match Rate 1	Match Rate 2	Total	Matched
Te3=24h vs Te6=24h	100%	100	100	100%	100%	100	100
Te6=24h vs Te9=24h	61%	164	100	61%	100%	164	100
Te3=24h vs Te9=24h	51%	137	70	51%	100%	137	70

Figure 3.11



Matching Summary for 'Te24h Matchset':

Member information

Get Name	Replicate Group	Spots	Matched	Match Rate 1	Match Rate 2	Corr Coeff	Detect param
Te3=24h (17c...	not assigned	187	88	51%	40%	0.872	Te24h paramete
Te6=24h (17c...	not assigned	214	214	100%	100%	1.000	Te24h paramete
Te9=24h (17c...	not assigned	137	84	61%	39%	0.716	Te24h paramete

Master is marked with * Correlation coefficient based on Te6=24h (17cm) ..

MatchSet information

Spots matched to every member:	59
Overall mean coefficient of variation:	45.24

Replicate group and classes information

Replicate Group/Classes	Member	Matched to all	Mean CV
all not assigned	3	59	45.24

Figure 3.12 Higher Level MatchSet- T0h and Te4h Comparison

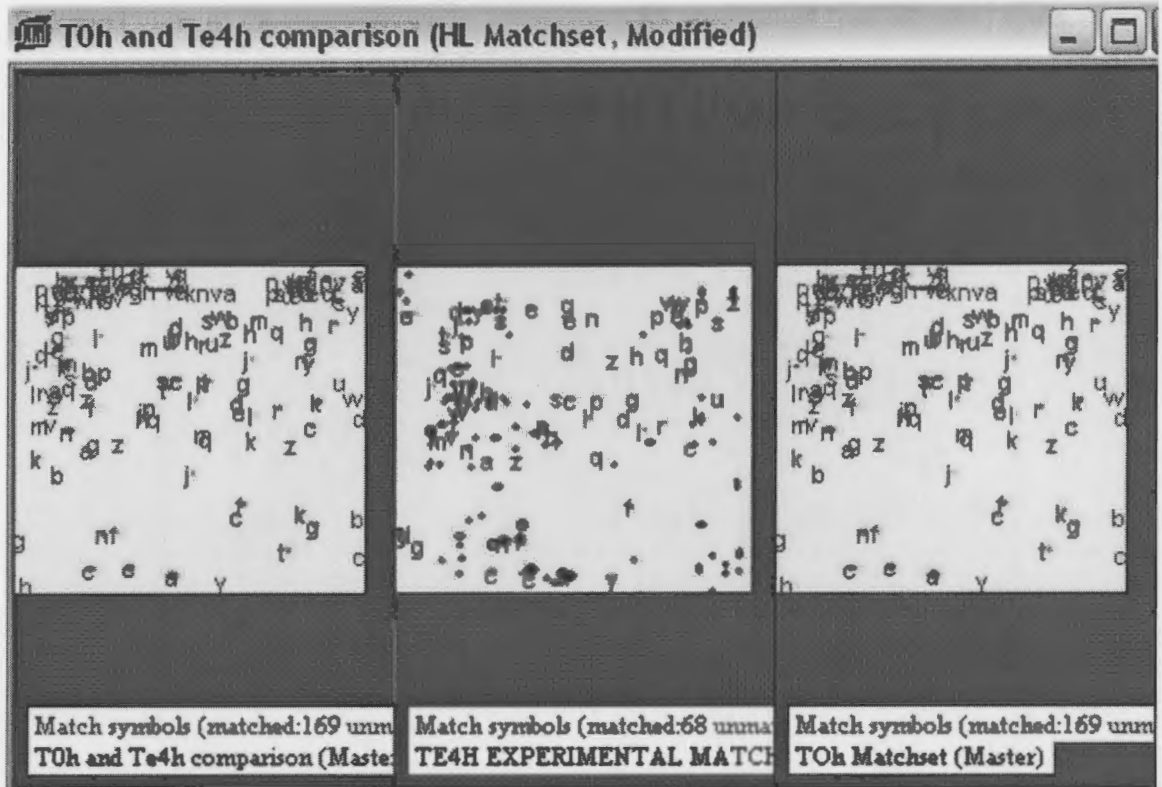
Represents Higher Level MatchSet created from T0h and Te4h primary MatchSets.

T0h MatchSet was chosen as the Master image. Yielded match rates: 100% and 43%. 85 spots were unmatched (red ellipses) while 68 spots were matched (green letters).



Matched	Unmatched	Total	Match Rate	Unmatch Rate	Total Spots	Matched Spots	Unmatched Spots
100%	0%	100%	100%	0%	85	85	0
43%	57%	100%	43%	57%	85	36	49

Figure 3.12 *Match Symbols (Matched: 68 unmarked) TE4H EXPERIMENTAL MATCHSET*



Matching Summary for 'TOh and Te4h comparison':

Member information							
Gal Name	Replicate Group	Spots	Matched	Match Rate 1	Match Rate 2	Corr Coeff	Detect paramet
TE4H EXPERIM...	not assigned	158	68	43%	38%	N/A	N/A
*TOh Matchset v1	not assigned	171	171	100%	100%	N/A	N/A

Master is marked with * Correlation coefficient based on N/A

MatchSet information		Replicate group and classes information		
Spots matched to every member:	68	Replicate Group/Classes	Member	Matched to all
Overall mean coefficient of variation:	N/A	all not assigned	2	68
				Mean CV
				N/A

Figure 3.13 Higher Level MatchSet-T0h and Te4h Comparison

Enlarged view of 68 matched (green letters) and 85 unmatched (red ellipses) spots.

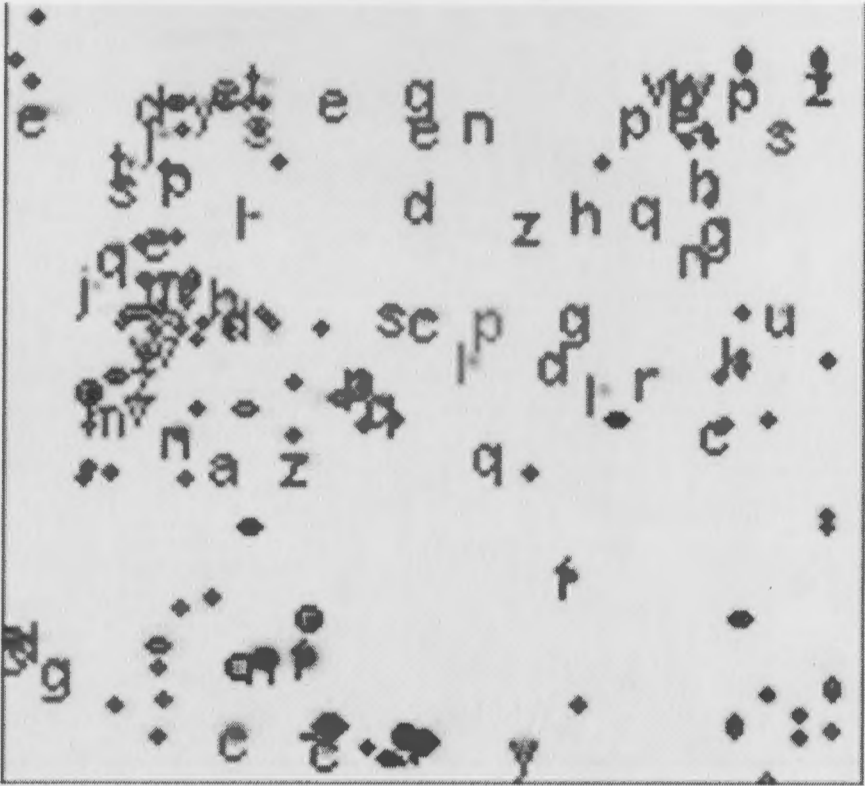


68 matched (green letters) 85 unmatched (red ellipses)

Figure 3.13 Higher Level Analysis: Comparison of T0h and Te4h

Enlarged view of 85 unmatched letters and red ellipses at Te4h testosterone-treated time point.

T0h and Te4h Comparison



68 matched (green letters) 85 unmatched (red ellipses)

Figure 3.14 Higher Level MatchSet-Unmatched spots

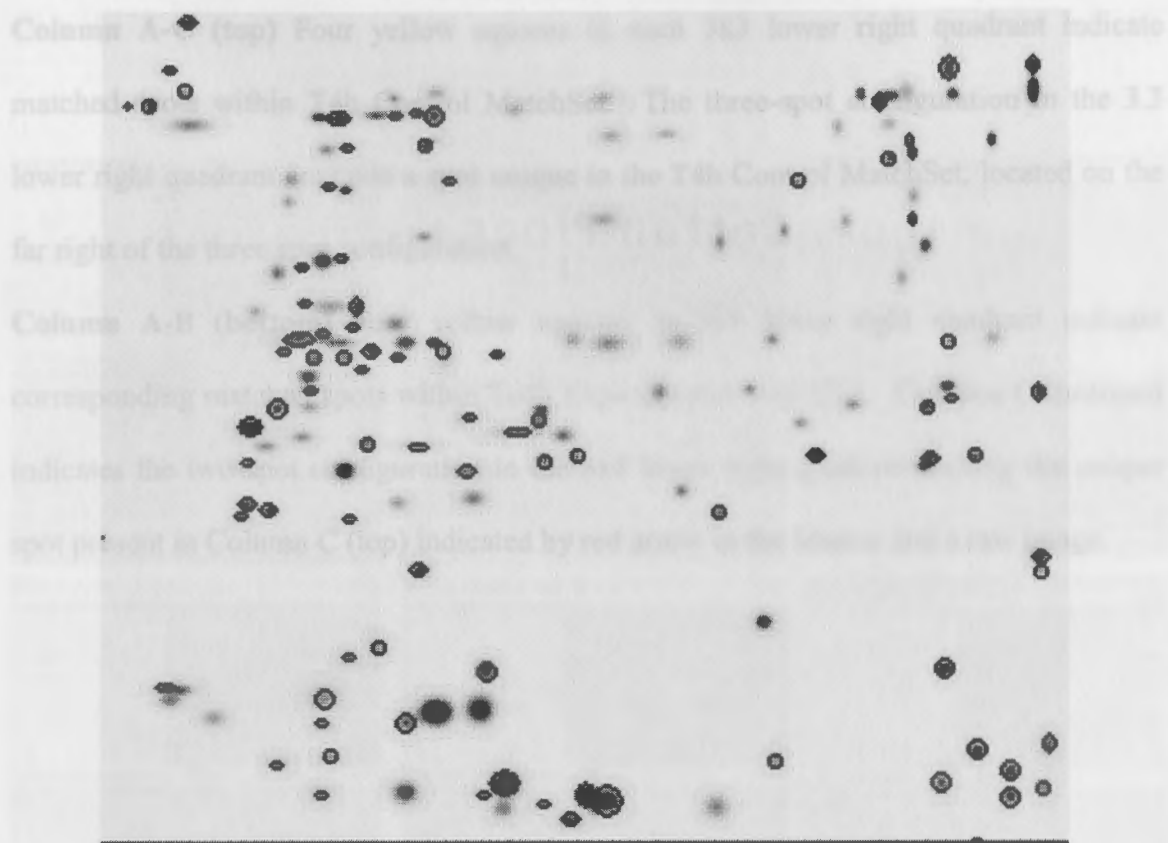
Enlarged view of 85 unmatched spots (red ellipses) unique to Te4h testosterone-treated time point.



85 Unmatched Spots

Figure 3.14 Manual Comparison of T4h Control and T4h Experimental

(Testosterone-treated) Match T0h and Te4h Comparison



85 Unmatched Spots

Figure 3.15 Manual Comparison of T4h Control and Te4h Experimental

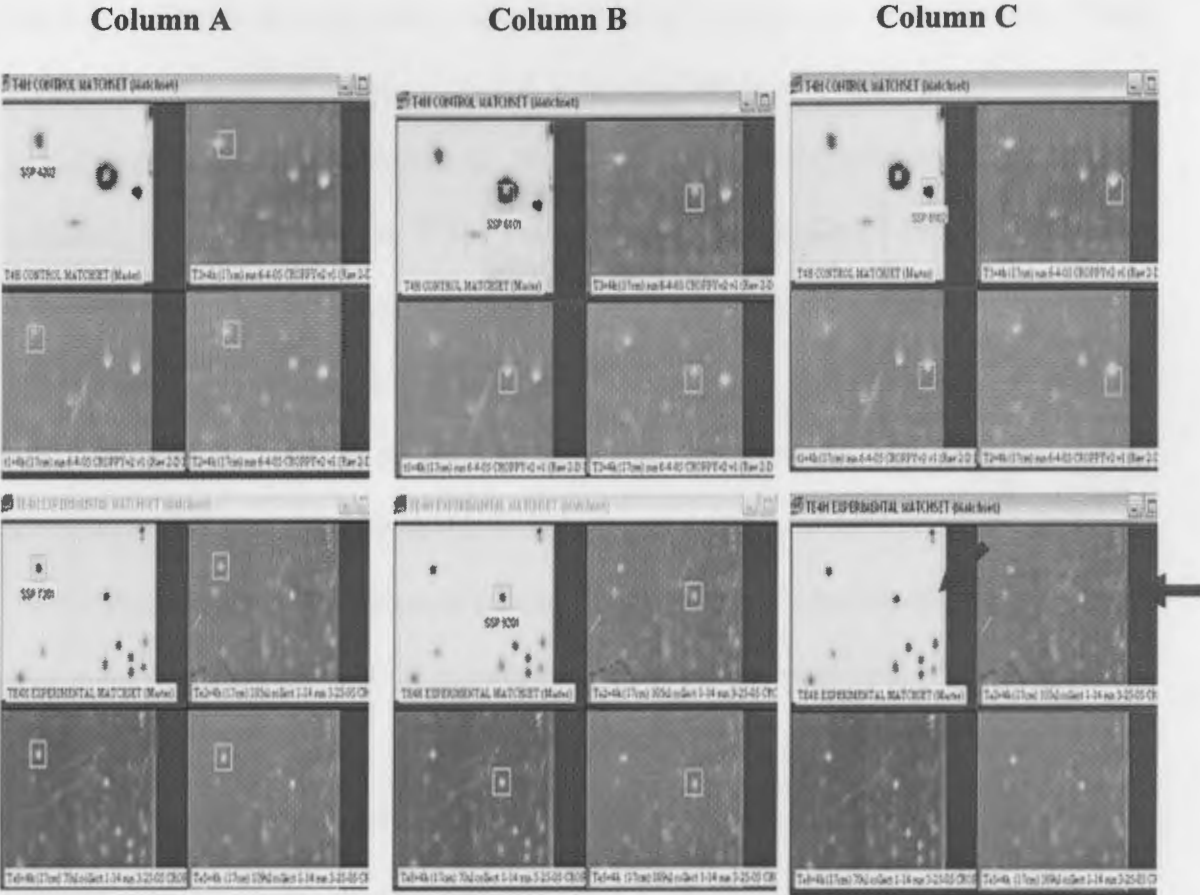
(Testosterone-treated) MatchSets

Column A-C (top) Four yellow squares in each 3x3 lower right quadrant indicate matched spots within T4h Control MatchSet. The three-spot configuration in the 3.3 lower right quadrant contains a spot unique to the T4h Control MatchSet, located on the far right of the three spot configuration.

Column A-B (bottom) Four yellow squares in 3x3 lower right quadrant indicate corresponding matched spots within Te4h Experimental MatchSet. **Column C (bottom)** indicates the two-spot configuration in the 3x3 lower right quadrant lacking the unique spot present in Column C (top) indicated by red arrow in the Master and a raw image.



Figure 3.15



The main goal of this proteomics-based study was to offer a comparative, combinatorial analysis of proteins expressed during differentiation of both testosterone-treated and untreated L2C12 myoblasts. Preliminary results have indicated differential proteins present in resulting protein spots identified by highly sensitive staining (Figure 3.13-3.15). Using the computer-based software, PDQuest™ 2-D Analysis Software, introductory information pertaining to the specified culture conditions has been achieved, based upon the identification of unique protein spots. Further analysis of proteins indicated would require excision of spots subjected to mass spectrometry, in which spots of interest are digested by enzymatic lysis and fragmented peptides identified. Database-search programs would then allow for the determination of exact amino acid sequences of testosterone-induced proteins.

CHAPTER IV:

DISCUSSION

Rudimentary application of PDQuest™ 2-D Analysis Software provided us with preliminary results as well as highlighting a need to improve its use. Following further examination of the PDQuest software, a better understanding of the vast array of features provided by the software will be gained. Initially, multiple trials using 7cm 2D-gels were scanned and subjected to PDQuest analysis. Parameter inconsistencies during the construction of MatchSets were discovered, requiring the usage of 17cm 2D-gels for adequate analyses of conditions.

The creation of MatchSets and Higher Level MatchSets created from lower-quality 17cm gels also proved problematic, due to an automatic inversion of spots edges due to spot quantities (Figure 3.8-3.9). However, PDQuest analyses of optimal-quality gels eased the identification of differential proteins as demonstrated in Figure 3.14 with 85 proteins unique to the 16th experimental time point. Further mass spectral analyses

The main goal of this proteomics-based study was to offer a comparative, combinatorial analyses of proteins expressed during differentiation of both testosterone-treated and untreated C2C12 myoblasts. Preliminary results have indicated differential proteins present in resulting protein maps visualized by highly sensitive staining (Figure 3.13-3.15). Using the computer-based analysis, PDQuest™ 2-D Analysis Software, introductory information pertaining to the specified cellular conditions has been achieved, based upon the identification of unique protein spots. Further analyses of proteins indicated would require excision of spots subjected to mass spectrometry, in which spots of interest are digested by enzymatic lysis and fragmented peptides identified. Database-search programs would then allow for the determination of exact amino acid sequences of testosterone-induced proteins.

Rudimentary application of PDQuest™ 2-D Analysis Software provided us with preliminary results as well as highlighting a need to improve its use. Following further examination of the PDQuest software, a better understanding of the vast array of features provided by the software will be gained. Initially, multiple trials using 7cm 2D-gels were scanned and subjected to PDQuest analysis. Parameter inconsistencies during the construction of MatchSets were discovered, requiring the usage of 17cm 2D-gels for adequate analyses of conditions.

The creation of MatchSets and Higher Level MatchSets created from lower-quality 17cm gels also proved problematic, due to an automatic inversion of spots edges due to spot quantities (Figure 3.8-3.9). However, PDQuest analyses of optimal-quality gels eased the identification of differential proteins as demonstrated in Figure 3.14 with 85 proteins unique to the Te4h experimental time point. Further mass spectral analyses

of the 85 differential proteins would offer more information pertaining to proteins expressed in the testosterone-treated state. The proteins may normally be expressed upon differentiation at the four hour time point, or quite possibly may be linked to testosterone administration of differentiating C2C12 cultures.

Manual comparison in combination with the PDQuest analyses also proved to be a useful technique for differential protein identification. As seen in Figure 3.15, when using the same parameters for cropping and detection, a protein configuration containing a spot unique to the T4h control time point was indicated. Because the spot was absent in the Te4h experimental time point, it is possible to hypothesize the function of that unknown protein. Perhaps under normal, untreated conditions, the protein is expressed at the four hour time point following induction of differentiation in C2C12 myoblasts, linked to cellular signaling associated with differentiation-specific regulatory factors. Consequently, it is possible that the expression of the protein would be delayed in C2C12 myoblasts as a result of the effects of testosterone on differentiation. The importance in delayed differentiation resulting from testosterone administration, lies in the extended time allotted for myoblast proliferation (cell cycle time). The extension of cell cycle time could ultimately aid in larger myotube formation, hence the increased muscle mass associated with testosterone administration (Orzechowski *et al.*, 2001).

Protein conformations present in resulting 2D-gel images following differentiation of C2C12 cultures in this study were similar to protein conformations present in 2D-gel images of total-cell proteins extracted from differentiating C2C12 cultures with the same pH gradient of 4-7 in another comparative proteomic study. However, the polyacrylamide gel percentage varied, eliminating the possibility for

manual comparison of spots. Because Tannu *et al.* identified several proteins involved in the proliferation and differentiation of C2C12 cultures, laying the foundation for further comparison, future work must be carried out to continue identifying proteins expressed as a result of varying conditions, such as in differentiating, testosterone-treated C2C12 cultures (Tannu *et al.*, 2004).

Future work contributing to the information obtained in this study requires further analyses of SYPRO[®] stained 17cm gels from both testosterone-treated and untreated conditions. Protein preparation should include a more reliable method of cell lysis and protein extraction, producing 2D-gels with higher match percentages in primary and Higher Level MatchSets. Extensive PDQuest analyses would facilitate the location of unique proteins for later excision and mass spectral analyses. Further information involving recommended exposure status, 2D-gel image parameter settings, crosshair placement, crop settings and matching tools would be helpful in the verification of differential proteins.

As reflected in this study, a proteomic-based approach in combination with known genomic information does indeed offer insight into unknown cellular processes such as myoblast differentiation and testosterone-effect analyses. Varying levels and intensities of protein expression may lead to identification of proteins associated with signaling cascades occurring as a result of specific cellular conditions. With the attainment of knowledge involving adult-tissue derived stem cells, therapies for degenerative diseases currently lacking effective treatments may be formulated.

References

1. Alberts B., Johnson A., Lewis J., Raff M., Roberts K., and P. Walter. (2002). *Molecular Biology of the Cell*. Garland Science 39 West 35th Street, New York, NY 10001-2299.
2. Abla A., Tabet C., James C., and R. Cysteux. (1992). Effect of Testosterone and Thyroid Hormone on the Expression of Myosin in the Sexually Dimorphic Levator Ani Muscle of Rat. *The Journal of Biological Chemistry* 267: 10052-10054.
3. Anzick J., and M. Mahaberoo. (2004). *Yeast two-hybrid in myotonic dystrophy*. *Developmental Biology* 267: 100-108.
4. Angele M., Nitach S., Knofler M., Ayala A., Angele P., Schüldberg F., Jauch K., and I. Chandry. Abstract (2003), *American Journal of Physiology Endocrinology and Metabolism* 285: E189-90.
5. Arnold A. M., Peralta J.M., and M. L. Thormay. (1997). Effect of Testosterone on Differential Muscle Growth and Nucleic Acid Concentrations in Muscles of Growing Lambs. *J. Anim. Sci.* 75: 1495-1502.
6. Betanova-Giorgianni, Sarka. (2003). Proteome analysis by two-dimensional gel electrophoresis and mass spectrometry: strengths and limitations. *Trends in Analytical Chemistry* 22:273-281.
7. Bery F.B., Mira Y., Mihara K., Kasper P., Sakita N., Hashimoto-Tanaka T., and T. Tomooka. (2001). Positive and Negative Regulation of Myogenic Differentiation of C2C12 Cells by Isoforms of the Multiple Homeodomain Zinc Finger Transcription Factor ATF1. *J. Biol. Chem* 276:25063-25065.
8. Bradford, M. M. (1976). A rapid and sensitive method for quantitation of microgram quantities of protein utilizing the principle of protein-dye binding. *Analytical Biochemistry* 72: 248.
9. Bruce G. J., and C. C. Hudson. (1987). Phosphorylation of the Translational Repressor Phos-1 by the Mammalian Target of Rapamycin. *Science* 277: 8056-8075.
10. Buffinger N., and F.E. Snockdale. (1995). Myogenic Specification of Sarcites is Mediated by Diffusible Factors. *Developmental Biology* 169: 96-108.
11. Cleveland D. W., Fischer S. G., Kirschner M. W., and U. K. Lammli. (1977). Peptide Mapping by Limited Proteinolysis in Sodium Dodecyl Sulfate and Analysis by Gel Electrophoresis. *The Journal of Biological Chemistry* 252: 1102-1106.

CHAPTER V:

REFERENCES

References

1. Alberts B., Johnson A., Lewis J., Raff M., Roberts K., and P. Walter. (2002). Molecular Biology of the Cell Garland Science 29 West 35th Street, New York, NY 10001-2299.
2. Albis A., Tobin C., Janmot C., and R. Couteaux. (1992). Effect of Testosterone and Thyroid Hormone on the Expression of Myosin in the Sexually Dimorphic Levator Ani Muscle of Rat. The Journal of Biological Chemistry 267: 10052-10054.
3. Amack J., and M. Mahadevan. (2004). Myogenic defects in myotonic dystrophy. Developmental Biology 265: 294-301.
4. Angele M., Nitsch S., Knoferl M., Ayala A., Angele P., Schildberg F., Jaunch K., and I. Chaundry. Abstract (2003). American journal of physiology Endocrinology and metabolism 285: E189-96.
5. Arnold A. M., Peralta J.M., and M. L. Thonney. (1997). Effect of Testosterone on Differential Muscle Growth and Nucleic Acid Concentrations in Muscles of Growing Lambs. J. Anim. Sci. 75: 1495-1503.
6. Beranova-Giorgianni, Sarka. (2003). Proteome analysis by two-dimensional gel electrophoresis and mass spectrometry: strengths and limitations. Trends in Analytical Chemistry. 22:273-281.
7. Berry F.B., Miura Y., Mihara K., Kaspar P., Sakata N., Hashimoto-Tamaoki T., and T. Tamaoki. (2001). Postive and Negative Regulation of Myogenic Differentiation of C2C12 Cells by Isoforms of the Multiple Homeodomain Zinc Finger Transcription Factor ATBF1. J. Biol Chem 276:25057-25065.
8. Bradford, M. M. (1976). A rapid and sensitive method for quantitation of microgram quantities of protein utilizing the principle of protein-dye binding. Analytical Biochemistry. 72: 248.
9. Brunn G. J., and C. C. Hudson. (1997). Phosphorylation of the Translational Repressor Phas-I by the Mammalian Target of Rapamycin. Science 277: 0036-8075.
10. Buffinger N., and F.E. Stockdale. (1995). Myogenic Specification of Somites Is Mediated by Diffusible Factors. Developmental Biology 169: 96-108.
11. Cleveland D. W., Fischer S. G., Kirschner, M. W., and U. K. Laemmli. (1977). Peptide Mapping by Limited Proteolysis in Sodium Dodecyl Sulfate and Analysis by Gel Electrophoresis. The Journal of Biological Chemistry 252: 1102-1106.

12. Candiano G. L., Musante, *et al.* (2002). Two-dimension maps in soft I immobilized pH gradient gels: A new approach to the proteome of the Third Millenium. Electrophoresis 23: 292-297.
13. Cross-Doerson D., and R. Isfort. (2003). A Novel Cell-Based System for Evaluating Skeletal Muscle Cell Hypertrophy-inducing agents. In Vitro Cell Dev. Biol.-Animal 39: 407-412.
14. Desler M., Jones S.J., Smith C.W., and T. L. Woods. (1996). Effects of Dexamethasone and Anabolic Agents on Proliferation and Protein Synthesis and Degradation in C2C12 Myogenic Cells. J. Anim. Sci. 74: 1265-1273.
15. Dinsmore J., Ratliff J., Deacon T., Pakzaban P., Jacoby D., Galpern W., and Isacson O. (1996). Cell Transplantation 5: 131-143.
16. Gal-Levi R., Leshem Y., Aoki S., Nakamura T., and O. Halevy. (1998). Hepatocyte growth factor plays a dual role in regulating skeletal muscle satellite cell proliferation and differentiation. Biochimica et Biophysica Acta 1402: 39-51.
17. Görg A., Weiss W., and M. J. Dunn. (2004). Current two-dimensional electrophoresis technology for proteomics (Review). Proteomics 4: 3665-3685.
18. Graves, Paul R., and Timothy A. J. Haystead. (2002). Microbiology and Molecular Biology Reviews 1: 2203-2215.
19. Ito H., MD, Hallauer P.L., PhD, Hastings K. E. M., PhD, and J. P. Tremblay, PhD. (1998). Prior Culture with Concanavalin A Increases Intramuscular Migration of Transplanted Myoblast. Muscle and Nerve 21: 291-297.
20. Joubert Y., Tobin C., and M. C. Lebart. (1993). Testosterone-induced Masculinization of the Rat Levator Ani Muscle during Puberty. Developmental Biology 162: 104-110.
21. Kadiyala S., Young R.G., Thiede M.A., and S.P. Bruder. (1997). Culture Expanded Canine Mesenchymal Stem Cells Possess Osteochondrogenic Potential In Vivo and In Vitro. Cell Transplantation 6: 125-134.
22. Kim D., Chi S., Ho Lee K., Rhee S., Kwon Y.K., Chung C.H., Kwon H., and M. S. Kang. (1999). Neuregulin Stimulates Myogenic Differentiation in an Autocrine Manner. J Biol Chem 274: 15394-15400.
23. Kitzmann M., and A. Fernandez. (2000). Crosstalk between cell cycle regulators and the myogenic factor MyoD in skeletal myoblasts. CMLS Cellular and Molecular Life Sciences 58: 571-579.

24. Lariviere, Andrew. (2002). Dexamethasone Increases Differentiation Capacity in C2C12 Cells and its Effects on Cdk1 and ERK1 Expression. *757*: 36.
25. Liu Y., Nifuji A., Tamura M., Wozney J., Olson E., and M. Noda (1997). Scleraxis Messenger Ribonucleic Acid Is Expressed in C2C12 Myoblasts and Its Level Is Down-Regulated by Bone Morphogenetic Protein-2 (BMP2). *Journal of Cellular Biochemistry* 67:66-74.
26. Lodish H, Berk A, Zipursky SL, Mattsdaire T, Baltimore D, and J. Darnell. (2000). Molecular Cell Biology, 4th Edition W.H. Freeman and Company, 41 Madison Avenue, New York, NY 10010
27. Loebel D.A. F., Watson C. M., Young A. D., and P. P.L. Tam. (2003). Lineage choice and differentiation in mouse embryos and embryonic stem cells. Developmental Biology 264: 1-14.
28. Mudali S., and A.S. Dobs. (2004). Effects of testosterone on body composition of the aging male. Mechanisms of Ageing and Development 125: 297-304.
29. Muller J.M., Isele U., Metzger E., Rempel A., Moser M., Pscherer A., Breyer T., Holubarsch C., Buettner R., and R. Schule. (2000). FHL2, a novel tissue-specific coactivator of the androgen receptor. The EMBO Journal 19:359-369.
30. Noguchi S., Tsukahara T., Fujita M, Kurokawa R., Tachikawa M., Toda T., Tsujimoto A., Arahata K., and I. Nishino. (2003). CDNA microarray analysis of individual Duchenne muscular dystrophy patients. Human Molecular Genetics 12: 595-600.
31. Okubo Y., Bessho K., Fujimara K., Iizuka T., and S. Mivatake. (1999). Expression of Bone Morphogenetic Protein-2 via Adenoviral Vector in C2C12 Myoblasts Induces Differentiation into the Osteoblast Lineage. Biochemical and Biophysical Research Communications 262: 739-743.
32. Orzechowski A., Grzelkwska K., Karlic W., and T. Motyl. (2001). Effect of Quercetin and DMSO on Skeletal Myogenesis from C2C12 Skeletal Muscle Cells with Special Reference to PKB/*Akt* Activity, Myogenin and Bcl-2 Expression. Basic Appl. Myol. 11: 31-44.
33. Roelen B.A.J., and P.T. Dijke. (2003). Controlling mesenchymal stem cell differentiation by TGF β family members. Journal of Orthopedic Science 8: 740-748.
32. Shen X., Collier J.M., Hlaing M., Zhang L., Delshad E.H., Bristow J., and H.S. Bernstein. (2003). Genome-Wide Examination of Myoblast Cell Cycle Withdrawal During Differentiation. Developmental Dynamics 226:128-138.

33. Sherwood, L. (1997). Human Physiology: From Cells to Systems Wadsworth Publishing Company, 10 Davis Drive, Belmont, CA 94002.
34. Singh R., Artaza J., Taylor W., Gonzalez-Cadavid N., and S. Bhasin. (2003). Androgens Stimulate Myogenic Differentiation and Inhibit Adipogenesis in C3H 10T1/2 Pluripotent Cells through an Androgen Receptor-Mediated Pathway. Endocrinology 144:5081-5018.
35. Skjaerlund D. M., Mulvaney D. R., Bergen W. G., and R. A. Merkel. (1994). Skeletal Muscle Growth and Protein Turnover in Neonatal Boars and Barrows. J. Anim. Sci. 72: 315-321.
36. Tannu, N. S., Rao, V. K., Chaudhary R. M., Giorgianni F., Saeed A. E., Goa Y., and R. Raghov. (2004). Comparative proteomes of the proliferating C₂C₁₂ Myoblasts reveal the complexity of the skeletal muscle differentiation program. Molecular & Cellular Proteomics 3: 1065-1082
37. te Pas, Marinus. F. W., de Jong, Pieter R., and Frans. J. Verburg. (2000). Glucocorticoid inhibition of C2C12 proliferation rate and differentiation capacity in relation to mRNA levels of the MRF gene family. Molecular Biology Reports 27:87-98.
38. Wada S., Yue L., and Furuta I. (2004) Oral Oncology 40: 164-169.
39. Yang S.Y., and G. Goldspink (2002). Different roles of the IGF-I Ec peptide (MGF) in myoblast proliferation and differentiation. Federation of European Biochemical Societies 522: 156-160.